

CALCAREOUS NANNOFOSSILS AND MESOZOIC OCEANIC ANOXIC EVENTS

Elisabetta Erba

Dipartimento di Scienze della Terra "A.Desio", Via Mangiagalli 34, 20133 Milano, Italy

Keywords: Calcareous nannofossils, Oceanic Anoxic Events, Jurassic, Cretaceous, palaeoceanography.

Abstract

Twenty-five years ago Mesozoic Oceanic Anoxic Events (OAEs) were documented and formalized as intervals of widespread to global deposition of organic matter. The Toarcian, early Aptian (OAE1a) and latest Cenomanian (OAE2) OAEs are truly global in nature, commonly carbonate-poor, and typically represented by organic carbon-rich black shales. In some areas, these OAEs are also characterized by abundant radiolarian-sands and silts. They are associated with negative and positive excursions in the $^{87}\text{Sr}/^{86}\text{Sr}$ record, in addition to large global carbon-isotope anomalies in carbonate and/or organic matter, caused by a major perturbation of the global carbon budget. Increased rates of volcanism during the formation of the Ontong Java (and Manihiki) and Caribbean Plateaus, and the Karoo-Ferrar Traps, are believed to have caused the geological responses associated with OAE1a, OAE2, and the Toarcian OAE, respectively. Excess volcanogenic CO_2 in the atmosphere most probably turned the climate into a greenhouse mode, accelerating continental weathering and increasing nutrient content in oceanic surface-waters *via* river run-off. Higher fertility in the global ocean was also probably triggered directly by submarine igneous events that introduced enormous quantities of biolimiting metals within hydrothermal plumes.

Because Mesozoic OAEs are often represented by carbonate-poor sediments, quantitative studies of calcareous nannofossils have been applied to explore (a) the causes and effects of igneous/tectonic events and climate changes, relative to nannofloral increases and crises, as well as (b) dissolution events and (c) diagenetic modifications. Characterization of calcareous nannofloras in OAE intervals can improve

our understanding of the marine ecosystem and biological processes such as photosynthesis (biological pump) and biomineralization (carbonate pump) that affect the organic and inorganic carbon cycle, as well as adsorption of atmospheric CO₂ in the oceans.

Types and rates of nanoplankton production and evolution are interpreted to trace the impact of major palaeoceanographic and palaeoclimatic events. In selected sections, it has been documented that calcareous nanofloras rapidly reacted to new conditions of fertility and higher *p*CO₂ by drastically reducing calcification. As in the modern oceans, during OAEs the increase of nutrients and atmospheric CO₂ induced higher abundances of nanoplankton producing small placoliths and inhibited the deep-photic zone nannoconids and schizosphaerellids.

Similarly to the 'nannoconid crisis' preceding deposition of the early Aptian OAE1a black shales, a 'schizosphaerellid crisis' is detected prior to the Toarcian OAE. Both OAEs are further characterized by a rapid nanofloral speciation, beginning approximately 1.5 my before OAE, but without extinctions. Global changes during the latest Cenomanian OAE 2 exerted different influences on calcareous nanoplankton that experienced a turnover due to most extreme environmental conditions. This event, in fact, was a time of extinctions followed by originations within calcareous nanofossils. Precise timing of the events before, during and after OAE1a, OAE2 and the Toarcian OAE indicate that they were intervals of enhanced oceanic productivity and that anoxia/dysoxia postdated biotic changes.

1. Introduction

In the early phases of ocean exploration, sediments exceptionally rich in organic carbon (Corg) were recovered from Cretaceous successions in the Pacific, Atlantic and Indian Oceans. Several of such black shales were proved coeval with similar lithologies outcropping in the Tethyan domain, suggesting widespread to global deposition of Corg – rich sediments during time-intervals named Oceanic Anoxic Events (OAEs) by

Schlanger and Jenkyns (1976). The original definition was based on lithological criteria, and applied to two time-intervals, namely the Aptian-Albian (OAE1) and Cenomanian-Turonian (OAE2). Subsequent investigations on land and in the oceans have identified the occurrence of the Coniacian-Santonian OAE3 (Jenkyns, 1980) and of the Toarcian OAE (Jenkyns, 1988).

Advances in stratigraphy have allowed a more precise dating of individual Corg-rich black shales, resulting in the subdivision of the long OAE1 interval into subevents, and a better dating of OAE2, OAE3, and the Toarcian OAE (Arthur et al., 1990; Jenkyns, 1999). Of all the OAEs, three are certainly global in nature, whereas other OAEs (OAE1b, OAE1c, OAE1d) have regional significance. The truly global Toarcian OAE, early Aptian OAE1a and latest Cenomanian OAE2 are represented by Corg-rich black shales, with extremely low or absent carbonate and locally abundant radiolarian layers (Jenkyns, 1999). The most spectacular sedimentary expression of the early Aptian and latest Cenomanian events are the Livello Selli and Livello Bonarelli, respectively. For both, the type-area is the Umbria-Marche Basin (central Italy), where a continuous hemipelagic to pelagic succession was deposited in the Jurassic to Paleogene interval.

Multidisciplinary investigations of pelagic sections representing OAE1a, OAE2 and the Toarcian OAE have resulted in the characterization of these episodes on the basis of sedimentology, palaeontology, as well as organic, inorganic and isotopic geochemistry. The Toarcian OAE, OAE1a and OAE2 are associated with large carbon-isotope excursions in carbonate and/or organic matter, caused by a major perturbation of the global carbon budget (Jenkyns, 1980; Jenkyns & Clayton, 1986, 1997; Weissert, 1989; Arthur et al., 1990; Bralower et al., 1993, 1994, 1999; Jenkyns et al., 1994; Erbacher et al., 1996; Menegatti et al., 1998; Weissert et al., 1998; Erba et al., 1999; Leckie et al., 2002). The temporal link between these events and major volcanic/tectonic episodes is testified to by large, positive and negative excursions in the $^{87}\text{Sr}/^{86}\text{Sr}$ curve reconstructed for the Jurassic and Cretaceous (see synthesis in Bralower et al., 1997; Jones & Jenkyns, 2001; Leckie et al., 2002).

Due to the biogenic nature of pelagic sediments representing OAEs, particular attention has been devoted to the biotic variations in planktonic communities associated with such episodes (Jarvis et al., 1988; Coccioni et al., 1992; Bralower et al., 1993, 1994; Larson et al., 1993; Erba, 1994; Claps et al., 1995; Erbacher et al., 1996, 2001; Bucefalo Palliani et al., 1998, 2002; Salvini & Marcucci Passerini, 1998; Hochuli et al., 1999; Paul et al., 1999; Premoli Silva et al., 1999; Leckie et al., 2002) to identify a sequence of palaeobiological changes before, during and after OAEs, and model the reactions of marine ecosystems to global changes.

In the Jurassic and Cretaceous oceans, the calcareous nannoplankton was the most efficient rock-forming group, whereas radiolarians were only temporarily important for lithogenesis under specific palaeoceanographic conditions (e.g. during the Middle Jurassic; Racki & Cordey, 2000). Planktonic foraminifers evolved in the Early Cretaceous and reached abundances relevant for lithogenesis only in the Late Cretaceous (Premoli Silva & Sliter, 1999). Although the appearance of diatoms is dated as Early Jurassic, this siliceous phytoplankton was never an important component in Jurassic and Cretaceous sediments (Fenner, 1995). Dinoflagellates were common and widely-distributed, but their preservation and abundance is strictly controlled by sedimentary facies and characteristics of bottom-waters, especially oxygen content (Tyson, 1995).

Jurassic and Cretaceous micrites mainly consist of coccoliths and nannoliths, in addition to variable amounts of diagenetic carbonate. Consequently, pelagic carbonates offer the opportunity of characterizing variations in abundance and composition of calcareous nannofloras, in addition to their relationships with changes in non-mineralizing phytoplankton and siliceous phytoplankton, as well as in calcareous and siliceous zooplankton (planktonic foraminifers and radiolarians). Because calcareous nannoplankton contribute to biological processes such as photosynthesis (biological pump) and biomineralization (carbonate pump), their increases in abundance and/or crises affect the inorganic and organic carbon cycle and adsorption of atmospheric CO₂ in the oceans. By analogy with living calcareous nannoplankton (Young, 1994),

morphology, size and ultrastructure of Jurassic and Cretaceous coccoliths and nannoliths can be used to trace ecological affinities and adaptations to temperature, chemistry and fertility of surface-waters (Erba and Tremolada, 2004).

This paper is focused on changes in calcareous nannofloral abundance and composition associated with the Toarcian OAE, OAE1a and OAE2. Published data and new results are integrated to propose a summary of nannofloral changes associated to OAEs. Analogies and differences will be discussed, and palaeoceanographic models will be proposed, in an attempt to unravel the preservation *versus* productivity enigma still debated for Jurassic and Cretaceous OAEs.

2. The Cretaceous OAEs

The mid-Cretaceous was a time of extreme climatic conditions, marked by a prolonged greenhouse mode (e.g. Jenkyns, 1999, 2003). The entire ocean/atmosphere system experienced a 'revolution' that is recorded in sedimentary successions at a global scale. It is not surprising that OAEs are concentrated in the Aptian-Turonian interval, when paroxysmal volcanic activity certainly affected the climate and the physico-chemical structure of the oceans (Larson, 1991a, 1991b; Kerr, 1998; Larson & Erba, 1999; Jenkyns, 1999; Leckie et al., 2002).

An overview of Cretaceous OAEs plotted against integrated stratigraphy, simplified $\delta^{18}\text{O}$ and $\delta^{13}\text{C}$ curves, and major submarine and subaerial volcanic events implicated in the constructions of Large Igneous Provinces (LIPs) is given in Figure 1. The early Aptian OAE1a and latest Cenomanian OAE2 correlates with the onset and climax of the mid-Cretaceous greenhouse climate, the most extreme warm episode in the past 150 My. Both OAEs are marked by a major decrease in the $^{87}\text{Sr}/^{86}\text{Sr}$ record (Bralower et al., 1997; Jones & Jenkyns, 2001), interpreted as the response to submarine volcanism during emplacement of the Ontong Java (and Manihiki) and Caribbean Plateaus, respectively. The large, positive excursions in the carbon-isotopes (up to 2‰ higher than background values) for both OAE1a and OAE2, are generally interpreted as due to accelerated burial of organic matter during episodes of enhanced productivity

(Weissert, 1989; Arthur et al., 1990; Weissert & Lini, 1991; Erba, 1994; Erbacher et al., 1996; Weissert et al., 1998; Jenkyns, 1999, 2003; Larson & Erba, 1999; Leckie et al., 2002).

Quantitative studies of pelagic successions reveal a major shift in the biogenic component, from carbonate-dominated to siliceous- and organic matter-dominated (Premoli Silva et al., 1999). Usually, calcareous nannofossils and foraminifers are abundant below and above black shales representing OAE1a and OAE2, when radiolarians and organic-walled microorganisms become overwhelming. Palaeontological evidence of meso- to eutrophic conditions support the productivity model forwarded for both OAE1a and OAE2 (Coccioni et al., 1992; Erba, 1994; Erbacher et al., 1996; Premoli Silva & Sliter, 1999; Salvini & Marcucci Passerini, 1998; Premoli Silva et al., 1999; Leckie et al., 2002). Changes in calcareous nannofossil assemblages are discussed below for the early Aptian OAE1a and latest Cenomanian OAE2, separately.

2.1 The early Aptian OAE1a

Within calcareous nannofossils, the 'nannoconid crisis' is the global event marking the early Aptian OAE1a (the Livello Selli; Erba, 1994). An earlier decrease in abundance of the rock-forming nannoconids has been documented slightly before magnetic chron CM0 and culminates with the crisis shortly, but unequivocally, preceding the deposition of black shales representing OAE1a (Figure 2). Such a change in nannofloral assemblages is documented worldwide (Bralower et al., 1993, 1994, 1999; Erba, 1994; Aguado et al., 1997, 1999; Channell et al., 2000; Bellanca et al., 2002; Bersezio et al., 2002; Erba & Tremolada, 2004) indicating that phytoplankton communities simultaneously reacted to a perturbation of the ocean/climate system. The nannoconid crisis is a typical example of the 'Lazarus effect' (Flessa & Jablonski, 1983) that terminated when more favourable conditions allowed re-occupation of nannoconid ecological niches. No extinctions within nannoconids, or nannofossils in general, have been documented in the OAE1a interval that is characterized by accelerated

evolutionary rates of nannoplankton. In fact, the onset of a nannofossil speciation episode starts approximately 1.5 my before OAE1a and continues through the late Aptian (Figure 2).

In the million years preceding OAE1a, planktonic foraminifers and radiolarians also increased in abundance, and assemblage composition gradually changed due to increasing percentages of *Globigerinelloides* and the Nassellaria (Coccioni et al., 1992; Premoli Silva et al., 1999). In the Livello Selli interval, representing OAE1a, Leupoldinids and Nassellaria dominate planktonic foraminiferal and radiolarian assemblages, respectively (Premoli Silva et al., 1999).

Leckie et al. (2002) describe OAE1a as a turnover, but I do not agree with this interpretation since calcareous plankton was not affected by extinctions. Late Aptian assemblages differ from early Aptian ones only because several new species (or morphotypes) of both calcareous nannoplankton and planktonic foraminifers appear (Premoli Silva et al., 1999). Also radiolarians are not affected by a typical turnover, because the sequence of first and last occurrences is diluted in a 1 my interval (Premoli Silva et al., 1999).

The changes in phytoplankton assemblages in the late Barremian – Aptian interval can be modelled using a three-fold subdivision as sketched in Figure 3. Phase one (124 to 121.5 M.a.) corresponds to phytoplankton assemblages in the Barremian ocean. Extending the interpretation of Erba (1994), it is here hypothesized that narrow-canal nannoconids lived in the lower photic zone, the wide-canal nannoconids inhabited the intermediate photic zone and coccolithophorids thrived in the upper photic zone. This model is based on size and weight of each group and supposed relationship between nannofossil mass and water depth: the heaviest forms were presumably adapted to the lower photic zone, while the lightest to the very surface. Because wide-canal nannoconids are smaller and lighter than the narrow-canal ones, perhaps their ecological niche was intermediate in the photic zone.

In the latest Barremian (phase 1; Figure 3) narrow-canal nannoconids were still the dominant forms, with minor proportions of wide-canal nannoconids and

coccoliths. The beginning of phase two is marked by the early changes within calcareous nannoplankton. Approximately 0.5 my before magnetic chron CM0 a coccolith speciation and a first decline in nannoconid relative and absolute abundance is detected (Erba, 1994; Erba et al., 1999; Larson & Erba, 1999; Premoli Silva et al., 1999; Channell et al., 2000; Erba & Tremolada, 2004). If the paleoecological interpretation of Erba (1994) is correct, then during the Barremian the nutricline was centered at the base of the thermocline favouring nannoconids in the deep photic zone. At magnetic chron CM0 time, a decrease in relative and absolute abundance of nannoconids coincided with a shift in dominance between the narrow- and the wide-canal forms (Erba, 1994; Erba et al., 1999; Larson & Erba, 1999; Premoli Silva et al., 1999; Channell et al., 2000; Erba & Tremolada, 2004). The latter become, for the first time, more abundant than the narrow-canal nannoconids, while coccolith abundance gradually increases upwards. The shift in dominance within nannoconids is interpreted as a response of calcareous nannoplankton to a rise of the nutricline accompanying a weakening of the thermocline due to initial warming of intermediate-waters in the early phase of the Ontong Java LIP. Based on carbon and oxygen isotopes on individual species of benthic and planktonic foraminifers, a similar scenario has been recently proposed for latest Albian OAE1d (Wilson & Norris, 2001). Submarine volcanism possibly further affected the trophic level of the oceans, by introducing iron and other biolimiting metals that are capable of triggering higher productivity, especially in oligotrophic areas (Larson & Erba, 1999; Leckie et al., 2002). Metal peaks were detected in magnetic chron CM0 suggesting a direct influence of igneous events on (calcareous) phytoplankton productivity (Larson & Erba, 1999; Leckie et al., 2002).

Phase three corresponds to the 'nannoconid crisis' characteristic of OAE1a. During the nannoconid crisis, coccoliths and peculiar nannoliths (*Assipetra* and *Rucinolithus*) were abundant within the calcareous nannoflora (Erba, 1994; Tremolada & Erba, 2002; Erba & Tremolada, 2004), and dinoflagellates and cyanobacteria became the dominant phytoplankton forms (Hochuli et al., 1999; Torricelli, 2000; van Bruegel et al., 2002) (Figure 3). At the onset of OAE1a, igneous/tectonic activity related to

emplacement of the giant Ontong Java and Manihiki Plateaus, and construction of the Nova Canton Trough, disrupted the thermal structure of the oceans by warming deep-, intermediate- and surface-waters, thus weakening and eventually eliminating the thermocline. Under such uniformly warm conditions, upwelling could have triggered and maintained high primary productivity (Wilson & Norris, 2001; Bice & Poulsen, 2002), further stimulated by continuous introduction of biolimiting metals at hydrothermal fields (Sinton & Duncan, 1997; Larson & Erba, 1999; Leckie et al., 2002) in addition to nutrient supply in coastal areas as river/eolian input. Oligotrophic nannoconids temporarily 'disappeared', but coccoliths continued to flourish, although dinoflagellates and cyanobacteria became dominant within phytoplankton (Hochuli et al., 1999; Larson & Erba, 1999; van Bruegel et al., 2002; Bralower et al., 2002; Figure 3).

Just after the OAE1a, the return of nannoconids has been documented worldwide (Erba, 1994; Bralower et al., 1994, 1999; Erba et al., 1999; Larson & Erba, 1999; Channell et al., 2000; Leckie et al., 2002; Erba & Tremolada, 2004), suggesting the restoration of the thermocline, deepening of the nutricline, and a general lowering of trophic levels. However, nannoconids never became as abundant as before OAE1a, although wide fluctuations in abundance characterize the late Aptian (Erba, 1994; Herrle, 2002; Leckie et al., 2002; Herrle & Mutterlose, 2003; Erba & Tremolada, 2004).

A synthesis of geological and biotic events that occurred in the latest Barremian-Aptian interval is illustrated in Figure 4. Changes in nannofossil assemblages testify to global perturbations in the ocean/atmosphere system during times of LIP formation. Prior, during and after OAE1a, the abundance and composition of calcareous nannoplankton as well as the dominance of various phytoplanktonic groups, seem strictly related to the thermal structure of the oceans (presence/absence and strength of the thermocline), trophic levels (oligo-, meso-, and eutrophic conditions), and atmospheric CO₂. Recently, nannofossil palaeofluxes have been estimated for the OAE1a interval in a well-dated section (Erba & Tremolada, 2004). A total decrease of approximately 90% in nannofossil paleofluxes occurred in a 1.5 m.y. long interval, at

the onset of the early Aptian C isotopic anomaly and OAE1a. Above the Selli Level, nannofossil paleofluxes recovered with an increase of approximately 60%. The nanoconid crisis might represent a combination of higher fertility and excess CO₂ that would both induce reduced biocalcification in calcareous nannoplankton (Erba and Tremolada, 2004).

Increasing percentages up to 60% of *Assipetra* and *Rucinolithus*, represented by normal- and large-sized morphotypes during OAE1a, are puzzling, because these nannoliths are quite big and heavily calcified (Tremolada & Erba, 2002) and contradict the biocalcification crisis hypothesis (Figure 4). Moreover, the volumes/mass and ultrastructure of *Assipetra* and *Rucinolithus* are totally different from those of the generally-accepted nannofossil indicators of higher surface water fertility. An alternative explanation might be that *Assipetra* and *Rucinolithus* are not fossil remains of coccolithophores, as further suggested by the lack of documentation of their coccospheres/xenospheres. I speculate that these peculiar nannoliths might represent CaCO₃ precipitates and/or biocalcification by bacteria under extreme palaeoenvironmental conditions, including massive methane release into the oceans (Opdyke et al., 1999, submitted; Tremolada & Erba, 2002; Bellanca et al., 2002; Beerling et al., 2002; Jenkyns, 2003).

2.2 The latest Cenomanian OAE2

Although the Cenomanian/Turonian OAE2 has been exhaustively studied in the past three decades, relatively little attention has been paid to changes in calcareous nannofossil assemblages. Since the pioneering work of Bralower (1988), quantitative investigations of nannofloras have been applied to a few sections, mostly from southern England (Jarvis et al., 1988; Lamolda et al., 1994; Paul et al., 1999; Gale et al., 2000). Changes in calcareous nannofloras are also documented for sections representing OAE2 in the Tethys Ocean (Paul et al., 1994; Lamolda & Gorostidi, 1996; Luciani & Cobianchi, 1999; Nederbragt & Fiorentino, 1999; Premoli Silva et al., 1999).

In Figure 5, the most significant changes in nannofossil assemblages in the well-studied Eastbourne section (southern England) are plotted against integrated stratigraphy, lithostratigraphy and carbon isotope stratigraphy. In the OAE2 interval, a relative decrease in total abundance and species richness was documented, but the striking feature is the major decrease in abundance of the fertility indicator *Biscutum constans*. This taxon is absent in the upper part of OAE2 and the immediately overlying sediments, whereas *Zeugrhabdotus erectus* is present throughout OAE2 (Jarvis et al., 1988; Lamolda et al., 1994; Paul et al., 1999). A similar trend was documented by Gale et al. (2000) for a fertility-index, based on the ratio between *Zeugrhabdotus* + *Biscutum* and *Watznaueria*.

Abundance peaks of *Eprolithus floralis* are documented at Eastbourne (Paul et al., 1999) and in other sections (Bralower, 1988; Lamolda & Gorostidi, 1996), suggesting cooler surface-waters in the late phase of OAE2 and immediately after it (Figure 5). This is in agreement with oxygen isotopic evidence for a reversed greenhouse effect after the thermal maximum coinciding with OAE2 (Clarke & Jenkyns, 1999; Jenkyns, 1999).

The OAE2 interval has also been studied for calcareous nannofossils at Gubbio (central Italy), considered the type-locality of the Livello Bonarelli (Erba, this study). Here, the whitish, pelagic limestones of the Scaglia Bianca are sharply interrupted by an approximately 1 m-thick black shale interval extremely enriched in organic matter, with abundant radiolarian layers, and carbonate-free (Figure 6; Arthur & Premoli Silva, 1982). Both nannofossil total abundance and species richness show a marked decrease in the interval preceding the Livello Bonarelli, where radiolarian layers and chert become the dominant lithology, and at the onset of the $\delta^{13}\text{C}$ positive excursion (Figure 6). Above the Livello Bonarelli, nannofloral abundance and species richness resumed, although values remain lower than in the interval preceding OAE2. The fertility indicators *Zeugrhabdotus* (*Z. erectus* and *Zeugrhabdotus* spp.) and *Biscutum constans* display different abundance distributions. While *Zeugrhabdotus* is present below and above the Livello Bonarelli, *Biscutum constans* has not been observed in the limestones

above the event (Figure 6). Both taxa are absent in the carbonate-free black shale interval, but *Zeugrhabdotus* is also absent in the limestones representing the latest phase of OAE2 as defined by C isotopes and then is present in the interval above OAE2, contrary to *Biscutum* that was not observed in the studied interval above the Livello Bonarelli.

In the latest Cenomanian, the gradual decrease in abundance of *Biscutum* is comparable to the trend at Eastbourne, although at Gubbio the absence of carbonates in the Livello Bonarelli prevents the documentation of the final decrease during the $\delta^{13}\text{C}$ maximum. A decrease in abundance of the fertility indicators *B. constans* and *Discorhabdus*, but not *Zeugrhabdotus*, in the OAE2 interval is also documented by Nederbragt & Fiorentino (1999) from Tunisia. These findings from distant localities suggest that the observed patterns are not induced by type of nannofloral preservation, and confirm the palaeoecological affinities of *Zeugrhabdotus* and *Biscutum* (as well as *Discorhabdus*) for different degrees of fertility, as previously hypothesized based on differential abundance patterns under meso- to eutrophic conditions (Watkins, 1989; Erba, 1992a, 1992b; Erba et al., 1992).

As observed at Eastbourne, abundance peaks of *Eprolithus floralis* (up to 40%) characterize the late phase of OAE2, suggesting cooler surface-waters reaching the Tethys Ocean. In the lower Turonian, nannoconids are present and their abundance fluctuates, reaching values as high as 10% (Figure 6).

The geological events and nannofossil changes associated with OAE2 are synthesized in Figure 7. Recent revision of radiometric dates for the Caribbean Plateau (Figure 6-1 by Larson et al. in Duncan & Bralower, 2002) confirms that a major submarine volcanism occurred in the Cenomanian/Turonian boundary interval (Arthur et al., 1985, 1987; Schlanger et al., 1987; Arthur et al., 1990; Sinton & Duncan, 1997; Kerr, 1998; Jenkyns, 1999; Wignall, 2001). The drop in the $^{87}\text{Sr}/^{86}\text{Sr}$ record, coincident with the beginning of the $\delta^{13}\text{C}$ excursion, strongly suggests a causal relationship between Caribbean LIP formation and the perturbation in the global carbon cycle. A direct link between submarine volcanism and changes in planktonic communities is

further supported by the occurrence of metal peaks just below and within sediments representing OAE2 at several localities (Brumsack, 1980; Arthur et al., 1990; Snow & Duncan, 2002; Turgeon et al., 2002). Although the decrease in abundance and species richness of calcareous nannofossils can be explained as the response of phytoplankton to higher concentrations of biolimiting metals (e.g., Fe, Zn) and nutrients, favouring siliceous and organic-walled groups (diatoms, dinoflagellates and cyanobacteria), the decline of nannofossil fertility indicators is puzzling. In fact, various independent parameters concur in the characterization of OAE2 as a high-productivity episode at global scale (Jenkyns, 1999). The *Biscutum* decline might represent trophic conditions above threshold values, and/or toxicity of specific metals, and/or inability to thrive in very warm waters. Previous studies on mid Cretaceous nannofloras indicated that *Biscutum* is indicative of mesotrophic, but not eutrophic conditions inducing increases in abundance of *Zeugrhabdotus* within calcareous nanoplankton (Erba, 1992a). It is unlikely that high water-temperature during the OAE2 thermal maximum (Clarke & Jenkyns, 1999; Jenkyns, 1999) inhibited *Biscutum*, because other species with a boreal affinity, such as *Zeugrhabdotus*, are present in the interval without *Biscutum*. Moreover, during the cooling episode at the end of OAE2, this taxon is not observed (Fig. 6).

The effects of metal toxicity are known for some extant nanoplankton species. For example cadmium inhibits calcification and copper is not tolerated by several coccolithophorid species (Brand, 1994). Perhaps in the Cretaceous, *Biscutum* suffered the presence of toxic metals introduced in large quantities via hydrothermal plumes (Sinton & Duncan, 1997; Duncan & Bralower, 2002; Erba & Duncan, 2002; Leckie et al., 2002). Metal toxicity might also explain the turnover affecting calcareous nannofossils, as expressed by a sequence of extinctions in a short time-interval (approximately 500 kyr), while originations start at the end of OAE2 and continue through the Turonian (Figure 7). Extreme palaeoenvironmental conditions possibly excluded the less well-adapted taxa, since most last occurrences affected short-ranging species. The origination of Turonian nannofossils is expressed mainly by appearance of new groups such as *Quadrum*. It is curious that these new genus is represented by

nannoliths that somehow resemble the Aptian *Assipetra* and *Rucinolithus* morphotypes, characteristics of OAE1a. In fact, although the ultrastructure of the individual genera is different, nannoliths of *Quadrum*, *Assipetra* and *Rucinolithus* are all blocky and highly calcified, when compared to common Cretaceous coccoliths.

3. The Toarcian OAE

Evidence for a Toarcian OAE (Jenkyns, 1985, 1988, 1999, 2003; Jenkyns & Clayton, 1986, 1997; Jenkyns et al., 2001) is limited to the boreal and tethyan areas, where Corg-rich black shales have been deposited in the *falciferum* and *serpentinus* ammonite Zones (see Bucefalo Palliani et al., 2002 for discussion of boreal and tethyan ammonite zonation). As for the Cretaceous OAEs, the Toarcian episode is marked by a pronounced decrease in carbonates, paralleled by an increase in organic matter and locally biosiliceous sedimentation (Gaetani & Poliani, 1978; Getani & Erba, 1990; Bucefalo Palliani et al., 1998; Jenkyns, 2003). The isotopic anomaly associated with the Toarcian OAE is marked by a negative $\delta^{13}\text{C}$ shift (*exaratum* ammonite Subzone) interrupting a positive carbon-isotope excursion dated as *tenuicostatum* to *falciferum* ammonite Zones (Hesselbo et al., 2000; Jenkyns, 2003). The negative shift has been interpreted as the result of methane release caused by global warming under greenhouse climatic conditions (Hesselbo et al., 2000; Beerling et al., 2002) caused by emplacement of the Karoo-Ferrar igneous province (Hesselbo et al., 2000; Wignall, 2001; Jenkyns, 2003). The Corg-rich black shales deposited during the Toarcian OAE have been interpreted as the result of increased primary productivity triggered by higher fluxes of nutrient from continents and intensified upwelling under greenhouse conditions (Jenkyns, 1999, 2003). Accelerated hydrological cycle and continental weathering is supported by the rise in $^{87}\text{Sr}/^{86}\text{Sr}$ and $^{187}\text{Os}/^{188}\text{Os}$ (Jones & Jenkyns, 2001; Cohen & Coe, 2002).

Quantitative studies of nannofossil assemblages through the Toarcian OAE interval are still limited (Mattioli, 1993; Bucefalo Palliani et al., 1998, 2002; Mattioli & Pittet, 2002), but a number of investigations can be used to trace a general picture of

calcareous nannoplankton changes during the Carixian to Aalenian interval (Noël et al., 1994; Claps et al., 1995; Picotti & Cobianchi, 1996; Mattioli, 1997; Cobianchi & Picotti, 2001). In pelagic sections from the Southern Alps a major lithologic change marks the lowermost Toarcian (lower part of the *tenuicostatum* ammonite Zone), namely a shift from Pliensbachian carbonate-rich lithologies to Toarcian marly lithologies (e.g. Gaetani & Erba, 1990; Cobianchi, 1992; Mattioli & Erba, 1999). Semiquantitative analyses and relative abundances (percentages) of nannofossil assemblages indicate that such a lithologic change corresponds to a drop in abundance of the rock-forming *Schizosphaerella* (Figures 8 and 9) (Picotti & Cobianchi, 1996; Cobianchi & Picotti, 2001; Erba, this study). This decrease in relative abundance is regarded here as a 'schizosphaerellid crisis', similar, although not as dramatic, to the nannoconid crisis described for OAE1a. Quantitative analyses of nannofossil assemblages indicate that absolute abundances of schizosphaerellids do not correlate to carbonate content (Mattioli & Pittet, 2002), and that *Schizosphaerella* is still dominant in the Toarcian (Bucefalo Palliani et al., 1998, 2002; Mattioli & Pittet, 2002).

As in the interval preceding the 'nannoconid crisis', the drop in schizosphaerellid relative abundance is anticipated by a nannoplankton speciation event that determined a general increase in abundance of coccoliths, as well as in species richness during the early Toarcian. The most striking variations in nannofossil assemblages occurred before the OAE. In fact, the nannoplankton speciation event is documented in both tethyan and boreal sections starting in the latest Pliensbachian *margaritatus* ammonite Zone (Figure 10) (Cobianchi et al., 1992; Bown et al., 1995; Bown & Cooper, 1998; Baldanza & Mattioli, 1999; Mattioli & Erba, 1999). Accelerated rates in nannofossil origination correlate with a decrease in the $^{87}\text{Sr}/^{86}\text{Sr}$ curve, and precede the onset of the C-isotope anomaly (Figure 10). It's worth mentioning that this speciation event mainly consists of appearances of various species of placoliths, possibly suggesting increasing surface water productivity conditions by analogy with Cretaceous findings.

The inverse correlation in relative abundances of coccoliths *versus* schizosphaerellids has also been documented at high frequencies in Toarcian-Aalenian

sections (Noël et al., 1994; Claps et al., 1995; Mattioli, 1997). This relationship, by analogy with extant and Cretaceous nannofossil assemblages, has been used to speculate that *Schizosphaerella* perhaps inhabited the lower part of the photic zone (Claps et al., 1995). In fact, the changes in schizosphaerellid/coccolith ratios in the Lower Jurassic are very similar to changes in nannoconid/coccolith ratios in the Lower Cretaceous and to changes in *Florisphaera profunda* /coccolith ratios in recent sediments.

Consequently, schizosphaerellids have been interpreted as oligotrophic forms flourishing in the lower part of the photic zone and reflecting a deep nutricline (Claps et al., 1995). A palaeoecologic affinity of *Schizosphaerella* for oligotrophic conditions has been confirmed by Picotti & Cobianchi (1996) and Cobianchi & Picotti (2001) based on pelagic as well as marginal sections close to carbonate platforms.

At both boreal and tethyan locations, the black shales representing the Toarcian OAE are usually depauperate in calcareous nannofossils and locally contain a peculiar palynological assemblage, dominated by *Tasmanites* (Bucefalo Palliani et al., 1998; 2002). In the Brown Moor section the temporary absence of calcareous nannofossils and dinoflagellate cysts in the interval corresponding to the negative $\delta^{13}\text{C}$ spike has been interpreted as a “disappearance event”, followed by a “repopulation event” (Bucefalo Palliani et al., 2002). Alternatively, the absence or extreme rarity of calcareous nannofossils during the negative $\delta^{13}\text{C}$ shift is here interpreted as the dissolution phase caused by clathrate melting (Hesselbo et al., 2000). This interpretation is also supported by the absence of extinctions. Very similar patterns are documented for calcareous nannofossil distributions in OAE1a. The negative spike at the base of the Livello Selli is, in fact, characterized by the absence-scarcity of nannofossils (and planktonic foraminifers) due to carbonate dissolution induced by methane release and oxidation of CO_2 , inducing CCD shallowing in the global ocean (Opdyke et al., 1999; submitted).

The Toarcian OAE is correlatable with formation of the Karoo-Ferrar Traps (Duncan et al., 1997; Palfy et al., 1997; Palfy & Smith, 2000; Wignall, 2001; Jenkyns, 2003), as also testified by the $^{87}\text{Sr}/^{86}\text{Sr}$ curve (Figure 11). This subaerial volcanism probably introduced high amounts of CO_2 in the atmosphere that triggered global

warming and increased continental weathering as well as nutrient transport into the oceans *via* river run-off (see Jenkyns, 2003 for a synthesis).

Changes in phytoplankton assemblages (Picotti & Cobianchi, 1996; Mattioli, 1993, 1997; Bucefalo Palliani et al., 1998, 2002; Cobianchi & Picotti, 2001; Mattioli & Pittet, 2002; Jenkyns, 2003; Erba, this study) are suggestive of higher fertility, enhanced primary productivity and consequent expansion of the oxygen minimum zone producing anoxia/dysoxia, as sketched in Figure 11.

If morphology, size and weight of calcareous nannoplankton reflect adaptation to specific ecological niches (Young, 1994), Early Jurassic nanofossils were probably distributed according to the physico-chemical and trophic characteristics of surface water-masses. As previously discussed for the Cretaceous, the heaviest forms were presumably adapted to the lower photic zone, intermediate forms to the middle photic zone, while the lightest to the very surface. Accordingly, it is here proposed that within the photic zone schizosphaerellids were the deepest forms, *Mitrolithus* and *Calyculus* inhabited the intermediate portion, and that placolith-bearing coccolithophores were the most superficial forms. Abundance of each group was dependent on the depth of the nutricline.

Based on the above interpretations, a regional model is here presented to explain nanofloral changes. In the late Pliensbachian (*spinatum* ammonite Zone), the presence of a deep nutricline centered at the thermocline favoured increases in abundance of *Schizosphaerella* and low relative abundance of all other nanofossils. An expanded and shallower nutricline at the beginning of the Toarcian (*tenuicostatum* ammonite Zone) favoured nannoplankton living in the intermediate (*Mitrolithus* and *Calyculus*) and upper (placoliths) photic zone, while opposing the deep schizosphaerellids. The nitrification episode persisted and intensified in the *falciferum* ammonite Zone as testified to by the positive $\delta^{13}\text{C}$ excursion, and global deposition of Corg-rich sediments characterized by organic walled and siliceous plankton (Jenkyns, 2003). The negative $\delta^{13}\text{C}$ shift, interrupting the positive excursion (Hesselbo et al., 2000; Jenkyns, 2003), represents extremely hostile paleoenvironmental conditions due to methane release that

hampered biocalcification and favoured tasmanitids (Bucefalo Palliani et al., 2002) and bacteria (Schouten et al., 2000; Jenkyns et al., 2001) (Figure 11). Dominance of *Tasmanites* in anoxic sediments and “marine peats” suggests that these cysts can survive in restricted and/or anaerobic habitats, even when all or most other organisms do not survive (Williams, 1978). At the same time, massive release of methane and oxygen consumption in the water-column altered the alkalinity of the ocean and strongly affected the benthic communities that experienced a mass extinction (see Wignall, 2001 for a synthesis).

4. Discussion and conclusions

Calcareous nannofossil assemblages display analogies and differences during the early Aptian OAE1a, latest Cenomanian OAE2 and the Toarcian OAE (Table 1). In these three cases, changes in abundance and composition precede the $\delta^{13}\text{C}$ anomaly and deposition of Corg-rich sediments (Erba, 1993). Therefore, nanoplankton responded to the early phases of palaeoenvironmental variations and continued to trace the perturbation in the ocean/atmosphere system during OAEs. Phytoplankton (and zooplankton) changes are here interpreted as the response of the biosphere to increasing fertility, culminating in the high-productivity event coincident with OAEs. A shift to meso- and eutrophic conditions in surface waters is supported by crises of the oligotrophic schizosphaerellids and nannoconids during the Toarcian OAE and OAE1a, respectively. Patterns of *Biscutum* and other nannofossil fertility indicators apparently contradict the productivity model proposed for OAE2. As stressed above, perhaps fertility became so high that only the most opportunistic nanoplankton taxa continued to thrive. Another explanation for the temporary absence of *Biscutum* and extinctions of several nannofossil taxa, might be excess quantities of toxic metals that affected specific coccolithophores. Because the nannoconid decline and crisis correlate with metal peaks, perhaps toxic metals might also have inhibited nannoconids in the late Barremian-early Aptian interval.

Since enhanced primary productivity is the most accepted explanation for OAE1a, OAE2 and the Toarcian OAE (see Jenkyns, 1999 for a synthesis), a mechanism capable of triggering eutrophism at a global scale must be found. Coastal nutrification due to increased continental weathering and run-off and/or local upwelling cannot explain high productivity documented in remote parts of large oceans during the early Aptian and latest Cenomanian. High-resolution studies of sedimentary successions representing OAE1a and OAE2 show trace-metal peaks coincident with major biotic changes reported before and during these events (Brumsack, 1980; Arthur et al., 1990; Larson & Erba, 1999; Snow & Duncan, 2002; Turgeon et al., 2002). Thus, increasing geological evidence suggests that OAE1a and OAE2 were mainly oceanic productivity events, largely controlled by submarine eruptions (Figure 12). Higher trophic levels were essentially induced and maintained by hydrothermal inputs of biolimiting metals (e.g., Fe, Zn) during the construction of the Ontong Java and Caribbean Plateaus, that also affected the ocean dynamics by warming deep- and intermediate-waters, causing more efficient nutrient cycling (warm upwelling) (Wilson & Norris, 2001; Bice & Poulsen, 2002).

Because there is no oceanic record *in situ* of the Toarcian OAE, high primary productivity might have occurred only in marginal environments due to coastal upwelling and nutrient transport by rivers into the oceans. This is the expected scenario during times of subaerial volcanism such as the formation of the Karoo-Ferrar Traps (Jenkyns, 1999). However, Monaco et al. (1999) report peculiar enrichments of trace metals in black shales representing the Toarcian OAE in central Italy. Such findings are possibly suggestive of metals resedimented from continents and/or a coeval submarine igneous event that might have introduced biolimiting metals causing changes in plankton productivity similar to those that occurred in the early Aptian and Cenomanian/Turonian boundary intervals. A drop in the $^{87}\text{Sr}/^{86}\text{Sr}$ curve close to the Pliesbachian/Toarcian boundary interval is consistent with the second hypothesis.

The three global OAEs are characterized by a carbonate crisis, both in pelagic and neritic environments, during times of extreme greenhouse conditions (Figure 12)

(Weissert et al., 1998; Cobianchi & Picotti, 2001; Herrle & Mutterlose, 2003). By analogy with extant communities, excess volcanogenic CO₂ most probably inhibited biocalcification in calcareous nannoplankton (see Riebesell et al., 2000) and planktonic foraminifers (Barker & Elderfield, 2002), as well as in reef communities (see Langdon et al., 2000). Carbonate sedimentation resumed after excess CO₂ was drawn down by accelerated weathering and burial of organic matter, and perhaps nutrient supply slowed down as well.

The negative spike at the base of the δ¹³C excursion, documented for both OAE1a and the Toarcian OAE, is interpreted as a massive methane release due to global warming (see Beerling et al., 2002 for a synthesis). In both cases, absence or rarity of calcareous nannofossils in sediments corresponding to the negative δ¹³C spike is interpreted as the dissolution event caused by methane melting and change in alkalinity hampering biocalcification and shallowing the CCD.

A negative δ¹³C shift has not been documented for OAE2, and consequently gas-hydrate melting did not concur with the perturbation of marine ecosystems in the Cenomanian/Turonian boundary interval, suggesting that methane release is not necessary for oceanic anoxia. The global carbonate decrease, expressed as deposition of large quantities of organic matter and temporarily biosiliceous sediments, was possibly caused by a combination of excess volcanogenic CO₂, preventing biocalcification in nannoplankton (and foraminifers), and eutrophic conditions favouring organic-walled and siliceous plankton.

Nannofossil evolutionary patterns are similar for the Toarcian OAE and OAE1a, which are both preceded by a speciation event and are not characterized by extinctions. On the contrary, a turnover characterizes nannofossil assemblages during OAE2, when several species disappeared, one after the other and then new species originated. The environmental perturbations during the Toarcian and the Aptian had, therefore, positive effects on calcareous nannoplankton and stimulated speciation. Perhaps much more extreme conditions during OAE2 negatively affected nannofloras.

Acknowledgements

This paper is the result of long and exciting discussions with friends and colleagues fascinated by oceanic anoxic events. A special note of thank goes to Hugh Jenkyns for sharing data and ideas, as well as support and advice. I'm also grateful to Helmi Weissert, Bob Duncan, Isabella Premoli Silva, Roger Larson, Brad Opdyke, and Paul Wilson for interesting discussions. Sincere thanks are extended to Stefano Poli for inspiring conversation on CO₂ and the global C cycle. The manuscript benefited from the reviews by Emanuela Mattioli, Jens Heerle and Jackie Lees: their constructive criticism and valuable suggestions were very helpful. This research was supported by COFIN 2001 to I. Premoli Silva and European Community's Improving Human Potential Programme contract HPRN-CT-1999-00055, C/T-Net.

References

- Aguado, R., Company, M., Sandoval, J., Tavera, J.M., 1997. Biostratigraphic events at the Barremian-Aptian boundary in the Betic Cordillera (Southern Spain). *Cret. Res.* 18, 309-329.
- Aguado, R., Castro, J.M., Company, M., de Gea, G.A., 1999. Aptian bio-events— an integrated biostratigraphic analysis of the Almadich Formation, Inner Prebetic Domain, SE Spain. *Cret. Res.* 20, 663-683.
- Arthur, M.A., Premoli Silva, I., 1982. Development of widespread organic carbon-rich strata in the Mediterranean Tethys. In: Schlanger, S.O., Cita, M.B. (Eds.), *Nature and origin of Cretaceous carbon-rich facies*. Academic Press, London, pp. 7-54.
- Arthur, M.A., Dean, W.E., Schlanger, S.O., 1985. Variations in global carbon cycling during the Cretaceous related to climate, volcanism, and changes in atmospheric CO₂. In: Sundquist, E.T., Broecker, W.S. (Eds), *The Carbon Cycle and Atmospheric CO₂: Natural Variations Archean to Present*. AGU Geophys. Monogr. 32, pp. 504-529.
- Arthur, M.A., Schlanger, S.O., Jenkyns, H.C., 1987. The Cenomanian-Turonian Oceanic Anoxic Event II, paleoceanographic controls on organic matter production and preservation. In: Brooks, J., Fleet, A. (Eds), *Marine Petroleum Source Rocks*. Geol. Soc. London Spec. Publ. 24, pp. 399-418.

- Arthur, M.A., Brumsack H.-J., Jenkyns, H.C., Schlanger, S.O., 1990. Stratigraphy, geochemistry, and paleoceanography of organic carbon-rich Cretaceous sequences. In: Ginsburg, R.N., Beaudoin, B. (Eds.), *Cretaceous Resources, Events, and Rhythms*. Kluwer Acad. Publ., pp. 75-119.
- Baldanza, A., Mattioli, E., 1999. Calcareous nannofossils. *Paleopelagos Spec. Publ.* 3, 107-111.
- Barker, S., Elderfield, H., 2002. Foraminiferal calcification response to glacial-interglacial changes in atmospheric CO₂. *Science* 297, 833–836.
- Beerling, D.J., Lomas, M.R., Gröcke, D.R., 2002. On the nature of methane gas-hydrate dissociation during the Toarcian and Aptian Oceanic Anoxic Events. *Am. Journ. Sci.* 302, 28-49.
- Bellanca, A., Erba, E., Neri, R., Premoli Silva, I., Sprovieri, M., Tremolada, F., Verga, D., 2002. Paleoceanographic significance of the Tethyan “Livello Selli” (Early Aptian) from the Hybla Formation, northwestern Sicily: biostratigraphy and high-resolution chemostratigraphic records. *Palaeogeogr. Palaeoclimatol. Palaeoecol.* 185, 175-196.
- Bersezio R., Erba E., Gorza M., Riva, A., 2002. Berriasian-Aptian black shales of the Maiolica formation (Lombardian Basin, Southern Alps, Northern Italy): local to global events. *Palaeogeogr. Palaeoclimatol. Palaeoecol.* 180, 253-275.
- Bice, K.L., Poulsen, C., 2002. Atmosphere and ocean circulation in a greenhouse world. In: Bice, K.L., et al. (Eds.) *Cretaceous climate-ocean dynamics: future directions for IODP*, http://www.whoi.edu/ccod/CCOD_report.htm.
- Bown, P.R., Cooper, M.K.E., 1998. Jurassic. In: Bown, P.R. (Ed.) *Calcareous nannofossil biostratigraphy*, British Micropalaeontological Society Publication Series, Kluwer Academic Publ., London, pp. 34-85.
- Bown, P. R., Baldanza, A., Bergen, J., Cobianchi, M., Cooper, K., Erba, E., Gardin, S., de Kaenel, E., Lozar, F., Mattioli, E., Monechi, S., Pirini Radrizzani, C., Reale, V., Roth, P., 1995. Recent advances in Jurassic calcareous nannofossil research. *GeoRes. For.* 1, 55-66.
- Bown, P.R., Rutledge, D.C., Crux, J.A., Gallagher, L.T., 1998. Lower Cretaceous. In: Bown, P.R. (Ed.) *Calcareous nannofossil biostratigraphy*, British Micropalaeontological Society Publication Series, Kluwer Academic Publ., London, pp. 86-131.
- Bralower, T.J., 1988. Calcareous nannofossil biostratigraphy and assemblages of the Cenomanian-Turonian boundary interval: implications for the origin and timing of oceanic anoxia. *Paleoceanography* 3, 275-316.
- Bralower, T.J., Sliter, W.V., Arthur, M.A., Leckie, R.M., Allard, D.J., Schlanger, S.O., 1993. Dysoxic/anoxic episodes in the Aptian-Albian (Early Cretaceous). In:

- Pringle, M. et al. (Eds.), *The Mesozoic Pacific: Geology, Tectonics and Volcanism*, AGU Geophys. Monogr. 77, pp. 5-37.
- Bralower, T. J., Arthur, M. A., Leckie, R. M., Sliter, W. V., Allard, D.J., Schlanger, S. O., 1994. Timing and paleoceanography of oceanic dysoxia/anoxia in the Late Barremian to Early Aptian. *Palaios* 9, 335-369.
- Bralower, T.J., Leckie, R.M., Sliter, W.V., Thierstein, H.R., 1995. An integrated Cretaceous microfossil biostratigraphy. *SEPM Spec. Publ.* 54, 65-79.
- Bralower, T. J., Fullagar, P. D., Paull, C. K., Dwyer, G. S., Leckie, R. M., 1997. Mid-Cretaceous strontium-isotope stratigraphy of deep-sea sections. *Geol. Soc. Am. Bull.* 109, 1421-1442.
- Bralower, T.J., CoBabe, E., Clement, B., Sliter, W.V., Osburne, C., Longoria, J., 1999. The record of global change in mid-Cretaceous, Barremian-Albian sections from the Sierra Madre, northeastern Mexico. *Journ. Foraminif. Res.* 29, 418-437.
- Bralower, T.J., Premoli Silva, I., Malone, M.J., et al., 2002. *Proceedings of the Ocean Drilling Program, Initial Reports, Volume 198: College Station, Texas, Ocean Drilling Program*, 148 pp.
- Brand, L.E., 1994. Physiological ecology of marine coccolithophores. In: Winter, A., Siesser, W.G. (Eds.), *Coccolithophores*. Cambridge Univ. Press, pp. 39–49.
- Brumsack, H.J., 1980. Geochemistry of Cretaceous Black Shales from the Atlantic Ocean (DSDP Legs 11, 14, 36, and 41). *Chem. Geol.* 31, 1-25.
- Bucefalo Palliani, R., Cirilli, S., Mattioli, E., 1998. Phytoplankton response and geochemical evidence of the lower Toarcian sea level rise in the Umbria-Marche basin (Central Italy). *Palaeogeogr. Palaeoclimatol. Palaeoecol.* 142, 33-50.
- Bucefalo Palliani, R., Mattioli, E., Riding, J.B., 2002. The response of marine phytoplankton and sedimentary organic matter to the early Toarcian (Lower Jurassic) oceanic anoxic event in northern England. *Mar. Micropaleontol.* 46, 223–245.
- Channell, J.E.T., Erba E., Muttoni G., Tremolada, F., 2000. Early Cretaceous magnetic stratigraphy in the APTICORE drill core and adjacent outcrop at Cismon (Southern Alps, Italy), and the correlation to the proposed Barremian/Aptian boundary stratotype. *Geol. Soc. Am. Bull.* 112, 1430–1443.
- Claps, M., Erba, E., Masetti, D., Melchiorri, F., 1995. Milankovitch-type cycles recorded in Toarcian black shales from the Belluno Trough (Southern Alps, Italy). *Mem. Sci. Geol. Padova* 47, 179–188.
- Clarke, L.J., Jenkyns, H.C., 1999. New oxygen isotope evidence for long-term Cretaceous climatic change in the Southern Hemisphere. *Geology* 27, 699-702.
- Cobianchi, M.A., 1992. Sinemurian-Early Bajocian calcareous nannofossil biostratigraphy of the Lombardy basin (Southern Calcareous Alps; Northern Italy). *Atti Ticinensi Sc. Terra* 35, 61-106.

- Cobianchi, M., Picotti, V., 2001. Sedimentary and biological response to sea-level and palaeoceanographic changes of a Lower-Middle Jurassic Tethyan platform margin (Southern Alps, Italy). *Palaeogeogr. Palaeoclimatol. Palaeoecol.* 169, 219-244.
- Cobianchi, M.A., Erba, E., Pirini-Radrizzani, C., 1992. Evolutionary trends of calcareous nannofossil genera *Lotharingius* and *Watznaueria* during the Early and Middle Jurassic. *Mem. Sci. Geol. Padova* 43, 19-25.
- Coccioni, R., Erba, E., Premoli Silva, I., 1992. Barremian-Aptian calcareous plankton biostratigraphy from the Gorgo a Cerbara section (Marche, central Italy) and implications for plankton evolution. *Cret. Res.* 13, 517-537.
- Coffin, M.F., Pringle, M.S., Duncan, R.A., Gladchenko, T.P., Storey, M., Muller, R.D., Gahagan, L.A., 2002. Kerguelen hotspot magma output since 130 Ma. *Journ. Petrol.* 43, 1121-1139.
- Cohen, A.S., Coe, A.L., 2002. The rhenium-osmium isotope system: applications to geochronological and palaeoenvironmental problems in the Mesozoic. Abstract Volume of Organic-carbon burial, climate change and ocean chemistry (Mesozoic-Paleogene), London, December 9-11, 2002, p. 8.
- Duncan, R.A., 2002. A time frame for construction of the Kerguelen Plateau and Broken Ridge. *Journ. Petrol.* 43, 1109-1119.
- Duncan, R.A., Bralower, T.J., 2002. Environmental and biotic consequences of large igneous provinces. In: Bice, K.L., et al. (Eds.) *Cretaceous climate-ocean dynamics: future directions for IODP*, http://www.whoi.edu/ccod/CCOD_report.htm.
- Duncan, R.A., Hooper, P.R., Rehacek, J., Marsh, J.S., Duncan, A.R., 1997. The timing and duration of the Karoo igneous event, southern Gondwana. *J. Geophys. Res. [Solid Earth]* 102, 18127-18138.
- Erba, E., 1992a. Middle Cretaceous calcareous nannofossils from the Western Pacific (ODP Leg 129): Evidence for paleoequatorial crossings. In: Larson, R.L., Lancelot, Y.(Eds.), *Proc. ODP Sci. Results* 129, 189-201.
- Erba, E., 1992b. Calcareous nannofossil distribution in pelagic rhythmic sediments (Aptian-Albian Piobbico core, central Italy). *Riv. Ital. Paleont. Strat.* 97, 455-484.
- Erba, E., 1993. Speciation of Mesozoic calcareous nannofossils forewarns anoxic events. *INA Newsl.* 15/2, 60-61.
- Erba, E., 1994. Nannofossils and superplumes: The early Aptian "nannoconid crisis," *Paleoceanography*, 9, 483-501.
- Erba, E., 1996. The Aptian Stage. *Bull. Inst. Royal Sci. Natur. de Belgique* 66 (suppl.), 31-43,
- Erba, E., Duncan, R.A., 2002. Geosphere-Biosphere Interactions and Mesozoic Oceanic Productivity Events. Abstract Volume of Organic-carbon burial, climate change and ocean chemistry (Mesozoic-Paleogene), London, December 9-11,

- 2002, p. 11.
- Erba, E., Tremolada, F., 2004. Nannofossil carbonate fluxes during the Early Cretaceous: Phytoplankton response to nitrification episodes, atmospheric CO₂, and anoxia. *Paleoceanography* 19, 10.1029/2003PA000884.
- Erba E., Castradori D., Guasti G., Ripepe M., 1992. Calcareous nannofossils and Milankovitch cycles: The example of the Albian Gault Clay Formation (Southern England). *Palaeogeogr. Palaeoclimatol. Palaeoecol.* 93, 47–69.
- Erba, E., Premoli Silva, I., Watkins, D., 1995. Cretaceous calcareous plankton biostratigraphy of Sites 872 through 879 (ODP Leg 144). In: Haggerty, J.A. et al. (Eds.), *Proc. ODP Sci. Results* 144, 157-169.
- Erba, E., Channell, J.E.T., Claps, M., Jones, C., Larson, R., Opdyke, B., Premoli Silva, I., Riva, A., Salvini, G., Torricelli, S., 1999. Integrated Stratigraphy of the Cismon APTICORE (Southern Alps, Italy): a “reference section” for the Barremian-Aptian interval at low latitudes. *Journ. Foraminif. Res.* 29, 371–392.
- Erba, E., Bartolini, A., Larson, R.L., 2004. Valanginian Weissert oceanic anoxic event. *Geology* 32, 149-152.
- Erbacher, J., 1994. Entwicklung und Palaeoozeanographie mittelkretazischer Radiolarien der westlichen Tethys (Italien) und des Nordatlantiks: Tuebinger Mikropalaeontologische Mitteilungen 12, 120 pp.
- Erbacher, J., Thurow, J., Littke, R., 1996. Evolution patterns of radiolaria and organic matter variations: A new approach to identify sea-level changes in mid-Cretaceous pelagic environments. *Geology* 24, 499-502.
- Erbacher, J., Huber, B.T., Norris, R.D., Markey, M., 2001. Increased thermohaline stratification as a possible cause for an oceanic anoxic event in the Cretaceous period. *Nature* 409, 325-327.
- Fenner, J., 1995. Late Cretaceous to Oligocene planktic diatoms. In: Bolli, H.M., Saunders, J.B., Perch-Nielsen, K. (Eds.) *Plankton stratigraphy*, Cambridge University press, pp. 713-762.
- Flessa, K.W., Jablonski, D., 1983. Extinction is here to stay. *Paleobiology* 9, 315-321.
- Gaetani, M., Erba, E., 1990. Il Bacino Lombardo: un sistema paleoalto/fossa in un margine continentale passivo durante il Giurassico. 75° Congresso nazionale S.G.I. Guida alle escursioni pre-Congresso, Escursione A3.
- Gaetani, M., Poliani, G., 1978. Il Toarciano e il Giurassico medio in Albenza (Bergamo). *Riv. Ital. Paleont. Strat.* 84, 349-382.
- Gale, A.S., Smith, A.B., Monks, N.E.A., Young, J.A., Howard, A., Wray, D.S., Huggett, J.M., 2000. Marine biodiversity through the Late Cenomanian-Early Turonian: palaeoceanographic controls and sequence stratigraphic biases. *Journ. Geol. Soc. London* 157, 745-757.

- Gradstein, F.M., Agterberg, F.P., Ogg, J.G., Hardenbol, J., Van Veen, P., Thierry, J., Huang, Z., 1995. A Triassic, Jurassic and Cretaceous time scale. *SEPM Special Publ.* 54, 95-126.
- Herbert, T.D., Fischer, A.G., 1986. Milankovitch climate origin of mid-Cretaceous black shale rhythms in central Italy. *Nature* 321, 739-743.
- Herrle, J.O., 2002. Paleooceanographic and Paleoclimatic Implications on Mid-Cretaceous Black Shale Formation in the Vocontian Basin and the Atlantic: Evidence from Calcareous nannofossils and Stable Isotopes, Tübingen *Mikropalaontologische Mitteilungen* 27, 114 pp.
- Herrle, J.O., Mutterlose, J., 2003. Calcareous nannofossils from the Aptian-early Albian of SE France: Paleooceanographic and biostratigraphic implications. *Cret. Res.* 24, 1-22.
- Hesselbo, S.P., Gröcke, D.R., Jenkyns, H.C., Bjerrum, C.J., Farrimond, P., Morgans Bell, H.S., Green, O.R., 2000. Massive dissociation of gas hydrate during a Jurassic oceanic event. *Nature* 406, 392-395.
- Hochuli, P., Menegatti, A.P., Riva, A., Weissert, H., Erba, E., Premoli Silva, I., 1999. High-productivity and cooling episodes in the early Aptian Alpine Tethys. *Geology* 27, 657-660.
- Jarvis, J., Carson, G.A., Cooper, M.K.E., Hart, M.B., Leary, P.N., Tocher, B.A., Horne, D., Rosenfeld, A., 1988. Microfossil Assemblages and the Cenomanian-Turonian (late Cretaceous) Oceanic Anoxic Event. *Cret. Res.* 9, 3-103.
- Jenkyns, H.C., 1980. Cretaceous anoxic events: From continents to oceans. *J. Geol. Soc. London*, 137, 171-188.
- Jenkyns, H.C., 1985. The early Toarcian and Cenomanian-Turonian anoxic events in Europe: comparisons and contrasts. *Geol. Rundsch.* 74, 505-518.
- Jenkyns, H.C., 1988. The Early Toarcian (Jurassic) anoxic event: stratigraphic, sedimentary, and geochemical evidence. *Am. Journ. Sci.* 288, 10-151.
- Jenkyns, H.C., 1999. Mesozoic anoxic events and paleoclimate. *Zbl. Geol. Paläont. Teil I*, 943-949.
- Jenkyns, H.C., 2003. Evidence for rapid climate change in the Mesozoic-Palaeogene greenhouse world. *Phil. Trans. Royal Soc., Series A*, 361, 1885-1916.
- Jenkyns, H.C., Clayton, C.J., 1986. Black shales and carbon isotopes in pelagic sediments from the Tethyan Lower Jurassic. *Sedimentology* 33, 87-106.
- Jenkyns, H.C., Clayton, C.J., 1997. Lower Jurassic epicontinental carbonates and mudstones from England and Wales: chemostratigraphic signals and the early Toarcian anoxic event. *Sedimentology* 44, 687-706.
- Jenkyns, H.C., Gale, A.S., Corfield, R.M., 1994. Carbon- and oxygen-isotope stratigraphy of the English Chalk and Italian Scaglia and its paleoclimatic significance. *Geol. Mag.* 131, 1-34.

- Jenkyns, H.C., Gröcke, D.R., Hesselbo, S.P., 2001. Nitrogen isotope evidence for water mass denitrification during the early Toarcian (Jurassic) oceanic anoxic event. *Paleoceanography* 16, 593-603.
- Jones, C.E., Jenkyns, H.C., 2001. Seawater strontium isotopes, Oceanic Anoxic Events, and seafloor hydrothermal activity in the Jurassic and Cretaceous. *Amer. Journ. Sci.* 301, 112-149.
- Kerr, A.C., 1998. Oceanic plateau formation: A cause of mass extinction and black shale deposition around the Cenomanian-Turonian boundary. *Jour. Geol. Soc. London* 155, 619-626.
- Kuypers, M.M.M., Pancost, R.D., Nijenhuis, I.A., Sinninghe Damsté, J.S., 2002. Enhanced productivity led to increased organic carbon burial in the euxinic North Atlantic basin during the late Cenomanian oceanic anoxic event. *Paleoceanography* 17, 3-13.
- Lamolda, M.A., Gorostidi, A., 1996. Calcareous nannofossils at the Cenomanian-Turonian Boundary Event in the Ganuza section, Northern Spain. In: Sahni, A. (Ed.), *Cretaceous Stratigraphy and Palaeoenvironments*. Geol. Soc. India, Mem. 37, 251-265.
- Lamolda, M.A., Gorostidi, A., Paul, C.R.C., 1994. Quantitative estimates of calcareous nannofossil changes across the Plenus Marls (latest Cenomanian), Dover, England: implications for the generation of the Cenomanian-Turonian Boundary Event. *Cret. Res.* 14, 143-164.
- Langdon, C., Takahashi, T., Sweeney, C., Chipman, D., Goddard, J., Marubini, F., Aceves, H., Barnett, H., Atkinson, M., 2000. Effect of calcium carbonate saturation state on the calcification rate of an experimental coral reef. *Glob. Geochem. Cycles* 14, 639-654.
- Larson, R.L., 1991a. Latest pulse of the Earth: Evidence for a mid Cretaceous super plume. *Geology* 19, 547-550.
- Larson, R. L., 1991b. Geological consequences of superplumes. *Geology* 19, 963-966.
- Larson, R. L., Erba, E., 1999. Onset of the mid-Cretaceous greenhouse in the Barremian-Aptian: Igneous events and the biological, sedimentary, and geochemical responses. *Paleoceanography* 14, 663-678.
- Larson, R.L., Fischer, A.G., Erba, E. and Premoli Silva, I., 1993. APTICORE-ALBICORE: A Workshop Report on Global Events and Rhythms of the mid-Cretaceous, 4-9 October 1992, Perugia, Italy, 56 pp.
- Leckie, R.M., Bralower, T.J., Cashman, R., 2002. Oceanic anoxic events and plankton evolution: Biotic response to tectonic forcing during the mid-Cretaceous. *Paleoceanography* 17, 10.1029/2001PA000623.

- Lini, A., 1994. Early Cretaceous carbon isotope stratigraphy of the Maiolica Formation, Southern Alps (Northern Italy and Southern Switzerland): stratigraphic and paleoenvironmental significance. Ph.D. Thesis, ETH Zurich, Switzerland, 259 pp.
- Luciani, V., Cobianchi, M., 1999. The Bonarelli Level and other black shales in the Cenomanian-Turonian of the northeastern Dolomites (Italy): calcareous nannofossil and foraminiferal data. *Cret. Res.* 20, 135-167.
- Mattioli, E., 1993. Quantitative analysis of calcareous nannofossils in the Liassic portion of Pozzale section (Martani Mts., Central Italy): preliminary report. *Paleopelagos* 3, 257-274.
- Mattioli, E., 1997. Nannoplankton productivity and diagenesis in the rhythmically bedded Toarcian-Aalenian Fiuminata section (Umbria-Marche Apennine, Central Italy). *Palaeogeogr. Palaeoclimatol. Palaeoecol.* 130, 113–133.
- Mattioli, E., Erba, E., 1999. Synthesis of calcareous nannofossil events in Tethyan Lower and Middle Jurassic successions. *Riv. Ital. Paleontol. Strat.* 105, 343–376.
- Mattioli, E., Pittet, B., 2002. Contribution of calcareous nannoplankton to carbonate deposition: a new approach applied to the Lower Jurassic of central Italy. *Mar. Micropaleontol.* 45, 175-190.
- Menegatti, A.P., Weissert, H., Brown, R.S., Tyson, R.V., Farrimond, P., Strasser, A., Caron, M., 1998. High-resolution $\delta^{13}\text{C}$ -stratigraphy through the early Aptian "Livello Selli" of the Alpine Tethys. *Paleoceanography* 13, 530-545.
- Monaco, P., Parisi, G., Ortega-Huertas, M., 1999. Geochemistry and clay minerals in the Early Toarcian. *Paleopelagos Spec. Publ.* 3, 127-129.
- Nederbragt, A.J., Fiorentino, A., 1999. Stratigraphy and palaeoceanography of the Cenomanian-Turonian Boundary Event in Oued Mellegue, north-western Tunisia. *Cret. Res.* 20, 47-62.
- Noël, D., Busson, G., Cornèe, A., Mangin, A.M., 1994. Le nannoplancton calcaire et la formation des alternances calcaires-marnes dans le Lias de Bassins de Marches-Ombrie (Italie). *Riv. Ital. Paleontol. Strat.* 99, 515-550.
- Opdyke, B.N., Erba, E., Larson, R.L., 1999. Hot Lips, methane and carbon isotope history of the Apticore, EOS, Transactions of the AGU, Fall Meeting, F486–487.
- Opdyke, B.N., Erba, E., Larson, R.L., Herbert, T.D., submitted. A history of methane hydrate release *and* formation gleaned from the detailed carbon isotope stratigraphy of the APTICORE, *submitted to Nature*
- Palfy, J., Smith, P.L., 2000. Synchrony between Early Jurassic extinction, oceanic anoxic event, and the Karoo-Ferrar flood basalt volcanism. *Geology* 28, 747-750.
- Palfy, J., Parrish, R.R., Smith, P.L., 1997. A U–Pb age from the Toarcian (Lower Jurassic) and its use for time scale calibration through error analysis of biochronologic dating. *Earth Planet. Sci. Lett.* 146, 659-675.

- Paul, C.R.C., Mitchell, S.F., Lamolda, M.A., Gorostidi, A., 1994. The Cenomanian-Turonian Boundary Event in northern Spain. *Geol. Mag.* 131, 801-817.
- Paul, C.R.C., Lamolda, M.A., Mitchell, S.F., Vaziri, M.R., Gorostidi, A., Marshall, J.D., 1999. The Cenomanian-Turonian boundary at Eastbourne (Sussex, UK): a proposed European reference section. *Palaeogeogr. Palaeoclimatol. Palaeoecol.* 150, 83-121.
- Picotti, V., Cobianchi, M., 1996. Jurassic periplatform sequences of the eastern Lombardian basin (Southern Alps). The deep-sea record of the tectonic evolution, growth and demise history of a carbonate platform. *Mem. Sci. Geol. Padova* 48, 171-219.
- Premoli Silva, I., Sliter, W.V., 1999. Cretaceous paleoceanography: Evidence from planktonic foraminiferal evolution. In: Barrera, E., Johnson, C.C. (Eds.), *The Evolution of Cretaceous Ocean-Climatic System*. *Geol. Soc. Am. Spec. Paper* 332, pp. 301-328.
- Premoli Silva, I., Erba, E., Salvini, G., Verga, D., Locatelli, C., 1999. Biotic changes in Cretaceous Anoxic Events. *Journ. Foraminifer. Res.* 29, 352-370.
- Racki, G., Cordey, F., 2000. Radiolarian palaeoecology and radiolarites: is the present the key to the past? *Earth Sci. Reviews* 52, 83-120.
- Renne, P.R., Glen, J.M., Milner, S.C., and Duncan, A.R., 2001, Age of Etendeka flood volcanism and associated intrusions in southwestern Africa. *Geology*, 24, 659-662.
- Riebesell, U., Zondervan, I., Rost, B., Tortell, P.D., Zeebe, R.E., Morel, F.M.M., 2000. Reduced calcification of marine plankton in response to increased atmospheric CO₂. *Nature* 407, 364-367.
- Salvini, G., Marcucci Passerini, M., 1998. The radiolarian assemblages of the "Bonarelli Horizon" in the Umbria-Marche Apennines and Southern Alps (Italy). *Cret. Res.* 19, 777-804.
- Schlanger, S.O., Jenkyns, H.C., 1976. Cretaceous oceanic anoxic events: Causes and consequences. *Geol. Mijnb.* 55, 179-184.
- Schlanger, S.O., Arthur, M.A., Jenkyns, H.C., Scholle, P.A., 1987. The Cenomanian-Turonian oceanic anoxic event, I. Stratigraphy and distribution of organic carbon-rich beds and the marine $\delta^{13}\text{C}$ excursion. In: Brooks, J., Fleet, J.A. (Eds.), *Marine Petroleum Source Rocks*, *Geol. Soc. London Spec. Publ.* 26, 371-399.
- Schouten, S., van Kaam Peters, H., Rijpstra, W.I.C., Schoell, M., Sinninghe Damsté, J., 2000. Effects of an oceanic anoxic event on the stable carbon isotopic composition of Early Toarcian carbon. *Am. J. Sci.* 300, 1-22.

- Sinton, C.W., Duncan, R.A., 1997. Potential links between ocean plateau volcanism and global ocean anoxia at the Cenomanian-Turonian boundary. *Econ. Geol.* 92, 836-842.
- Snow, L.J., Duncan, R.A., 2002. Hydrothermal Links Between Ocean Plateau Formation and Global Anoxia, Abstract Volume of the Workshop on Cretaceous Climate and Ocean Dynamics, Florissant, Colorado, July 14-18, 2002, p. 74.
- Torricelli, S., 2000. Lower Cretaceous dinoflagellat cyst and acritarch stratigraphy of the Cismon Apticore (Southern Alps, Italy). *Rev. Palaeobot. Palynol.* 108, 213-266.
- Tremolada, F., Erba, E., 2002. Morphometric analysis of the Aptian *Rucinolithus terebrodentarius* and *Assipetra infracretacea* nannoliths: implications for taxonomy, biostratigraphy and paleoceanography. *Mar. Micropaleont.* 44, 77-92.
- Tsikos, H., Jenkyns, H.C., Walsworth-Bell, B., Petrizzo, M.R., Forster, A., Kolonic, S., Erba, E., Premoli Silva, I., Baas, M., Wagner, T., and Sinninghe Damsté, J.S, in press. Carbon-isotope stratigraphy recorded by the Cenomanian/Turonian Oceanic Anoxic Event: correlation and implications based on three key-localities. *Journ. Geol. Soc. London.*
- Turgeon, S., Brumsack, H.J., Kuypers M., Böttcher, M.E., 2002. How extreme can you get? A closer look at sediment geochemistry of the Upper Cenomanian and lower Turonian at Gubbio and Furlo in Italy. Abstract Volume of Organic-carbon burial, climate change and ocean chemistry (Mesozoic-Paleogene), London, December 9-11, 2002, p. 19.
- Tyson, R.V., 1995. Sedimentary organic matter. Chapman & Hall, London, UK, 615 pp.
- van Bruegel, Y., Schouten, S., Erba, E., Price, G.D., Sinninghe Damsté, J., 2002. The global Aptian Selli Event: Molecular examination of the negative carbon isotope spike. Abstract Volume of Organic-carbon burial, climate change and ocean chemistry (Mesozoic-Paleogene), London, December 9-11, 2002, p. 19.
- Watkins, D.K., 1989. Nannoplankton productivity fluctuations and rhythmically-bedded pelagic carbonates of the Greenhorn Limestone (Upper Cretaceous). *Palaeogeogr. Palaeoclimatol. Palaeoecol.* 74, 75-86.
- Weissert, H., 1989. C-isotope stratigraphy, a monitor of paleoenvironmental changes: a case study from the Early Cretaceous. *Surv. Geoph.* 10, 1-16.
- Weissert, H., Lini, A., 1991. Ice age interlude during the time of Cretaceous greenhouse climate?. In: Müller, D.W., McKenzie, J.A., Weissert, H. (Eds.), *Controversies in Modern Geology*, Academic Press, London, pp. 173-191.
- Weissert, H., Lini, A., Föllmi, K.B., Kuhn, O., 1998. Correlation of Early Cretaceous carbon isotope stratigraphy and platform drowning events: A possible link?, *Palaeogeogr. Palaeoclimatol. Palaeoecol.* 137, 189-203.

- Wignall, P.B., 2001. Large igneous provinces and mass extinctions. *Earth Sci. Rev.* 53, 1-33.
- Williams, G.L., 1978. Dinoflagellates, Acritarchs and Tasmanitids. In: Haq, B.U., Boersma, A. (Eds.), *Introduction to marine micropaleontology*. Elsevier, New York, pp. 293-326.
- Wilson, P. A., Norris, R. D., 2001. Warm tropical ocean surface and global anoxia during the mid-Cretaceous period. *Nature* 412, 425-429.
- Young, J.R., 1994. Functions of coccoliths. In: Winter, A., Siesser, W.G. (Eds.), *Coccolithophores*. Cambridge Univ. Press, Cambridge, pp. 63-82.

FIGURE and TABLE CAPTIONS

- Fig. 1. Cretaceous OAEs plotted against magneto-, bio- and chemo-stratigraphy. Nannofossil and planktonic foraminiferal biostratigraphy after Bralower et al. (1995), Erba et al. (1995), Premoli Silva & Sliter (1999). Simplified $\delta^{18}\text{O}$ and $\delta^{13}\text{C}$ curves after Lini (1994), Erbacher (1994), Jenkyns et al. (1994), Menegatti et al. (1998), Weissert et al. (1998), Clarke & Jenkyns (1999), Erba et al. (1999), Herrle (2002). Timescale after Gradstein et al. (1995). Duration of OAEs: Weissert OAE after Erba et al. (2004), OAE1a after Opdyke et al. (submitted), OAE1b after Herrle (2002), OAE1c after (Herbert & Fischer, 1986), OAE1c after Wilson & Norris (2001), OAE2 after Kuypers et al. (2002).
- Fig. 2. Synthesis of major biotic and geological events in the late Barremian-Aptian interval. Nannofossil speciation: 1 = FO of *F. oblongus*, 2 = FO of *R. irregularis*, 3 = FO of *R. gallagheri*, 4 = FO of *N. truittii*, 5 = FO of *A. infracretacea larsonii*, 6 = FO of *R. terebrodentarius youngii*, 7 = FO of *R. angustus*, 8 = FO of *F. varolii*, 9 = FO of *E. floralis*, 10 = FO of *R. planus*, 11 = FO of *C. acutum*, 12 = FO of *B. hockwoldensis*, 13 = FO of *B. africana*, 14 = FO of *D. striatus* (after Bralower et al., 1995; Erba, 1996; Bown et al., 1998; Herrle, 2002).
- Fig. 3. Phytoplankton changes in the latest Barremian – early Aptian interval (OAE1a).
- Fig. 4. Synthesis of nannofossil changes across the early Aptian OAE1a. Timescale after Gradstein et al. (1995); $\delta^{13}\text{C}$ curve after Erba et al. (1999) and Weissert et al. (1998); $^{87}\text{Sr}/^{86}\text{Sr}$ curve after Jones & Jenkyns (2001); ages of Ontong Java Plateau (=OJP) and Kerguelen LIP after Larson & Erba (1999) and Duncan (2002); Metal peaks after Larson & Erba (1999) and Duncan (pers.comm.); nannofossil paleofluxes and pCO_2 after Erba & Tremolada (2004); other nannofossil events after Erba (1994) and Tremolada & Erba (2002).
- Fig. 5. Changes in nannofossil total abundance and species richness, percentages of *Biscutum*, variations of the fertility index and abundance peaks of *E. floralis* in the OAE2 interval of the Eastbourne area (southern England) (after Lamolda et al., 1994; Paul et al., 1999; Gale et al., 2000), plotted against litho, bio-, and C isotopic stratigraphy. Lithostratigraphy (chalk intervals are shown as white,

marls as stippled) and ammonites after Gale et al. (2000); $\delta^{13}\text{C}$ curve, nannofossil and planktonic foraminiferal biostratigraphy after Tsikos et al. (in press).

Fig. 6. Changes in nannofossil abundance and species richness and percentages of *Biscutum*, *Zeugrhabdotus*, *Nannoconus* and *E. floralis* in the OAE2 interval at Gubbio (central Italy), plotted against litho, bio-, and C isotopic stratigraphy. $\delta^{13}\text{C}$ curve, nannofossil and planktonic foraminiferal biostratigraphy after Tsikos et al. (in press)

Fig. 7. Synthesis of nannofossil changes across the latest Cenomanian OAE2. Nannofossil and planktonic foraminiferal biostratigraphy after Bralower et al. (1995) and Erba et al. (1995). Timescale after Gradstein et al. (1995); $^{87}\text{Sr}/^{86}\text{Sr}$ curve after Jones and Jenkyns (2001); age of Caribbean Plateau after Duncan & Bralower (2002); metal peaks after Turgeon et al. (2002) and Turgeon (pers.comm.); nannofossil events after Paul et al. (1999), Gale et al. (2000), and Erba (this study).

Fig. 8. Nannofossil changes in the Pliensbachian-Aalenian interval of the Breggia section (after Picotti & Cobianchi, 1996).

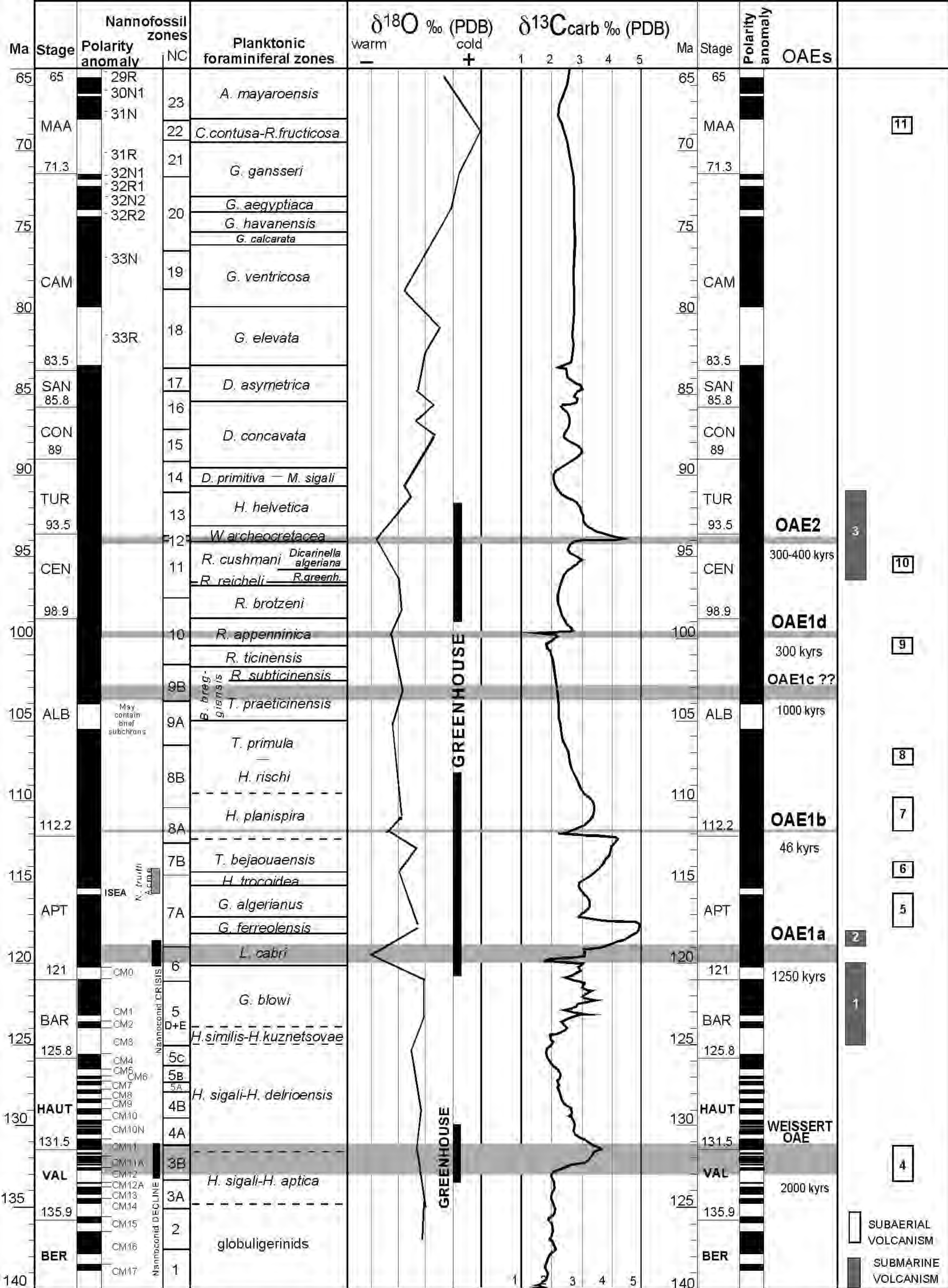
Fig. 9. Nannofossil changes in the Pliensbachian-Aalenian interval of the Colle di Sogno section (Erba, this paper). $\delta^{13}\text{C}$ and $\delta^{18}\text{O}$ curves after Jenkyns & Clayton (1986).

Fig. 10. Synthesis of nannofossil changes across the Toarcian OAE. Nannofossil speciation: 1 = FO of *B. finchii*, 2 = FO of *L. hauffii*, 3 = FO of *L. barozii*, 4 = FO of *Calyculus* spp., 5 = FO of *L. sigillatus*, 6 = FO of *C. poulabronei*, 7 = FO of *C. cantaluppii*, 8 = FO of *C. crucicentralis*, 9 = FO of *C. superbus*, 10 = FO of *L. velatus*, 11 = FO of *D. ignotus*, 12 = FO of *W. colacicchii*, 13 = FO of *W. fossacineta*, 14 = FO of *D. striatus* (after Mattioli and Erba, 1999). Timescale after Gradstein et al. (1995); age of Karoo-Ferrar Traps after Duncan et al. (1997), Palfy et al. (1997) and Wignall (2001).

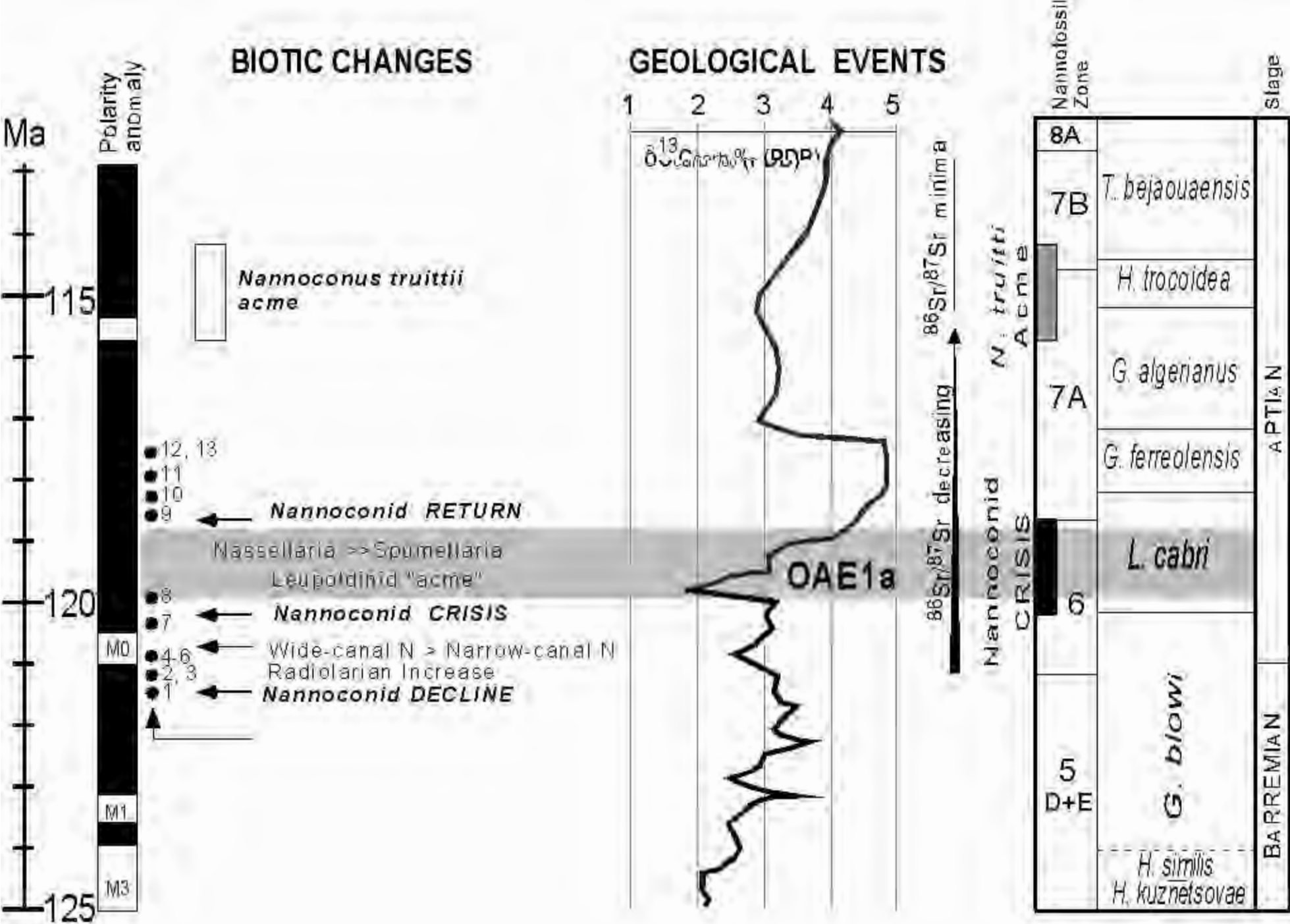
Fig. 11. Phytoplankton changes in the late Pliensbachian-early Toarcian interval (Toarcian OAE).

Fig. 12 . Processes that might relate igneous events to biological and geological responses eventually recorded in marine sediments. Modified after Larson & Erba (1999).

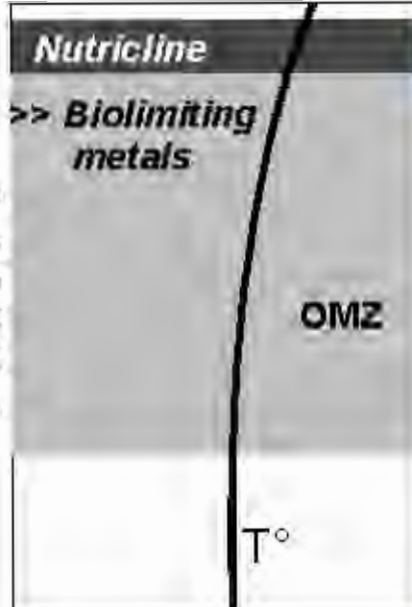
Table 1. Comparison of OAE2, OAE1a and the Toarcian OAE. Duration of OAEs: OAE1a after Opdyke et al. (submitted), OAE2 after Kuypers et al. (2002), Toarcian OAE after Hesselbo et al. (2000).



IGNEOUS EVENTS: 1 = Ontong Java and Manihiki Plateaus (Larson & Erba, 1999); 2 = ODP Site 1136, Kerguelen Plateau (Coffin et al., 2002); 3 = Caribbean Plateau (Larson et al., 2002); 4 = Parana-Etendeka (Renne et al., 2001); 5 = Rajmahal Traps (Coffin et al., 2002); 6 = laprophyre dikes of the conjugate Indian and Antarctic margins (Coffin et al., 2002); 7 = northern Kerguelen Plateau (Coffin et al., 2002); 8 = Elan Bank (Coffin et al., 2002); 9 = central Kerguelen Plateau (Coffin et al., 2002); 10 = Broken Ridge (Coffin et al., 2002); 11 = Skiff Bank (Coffin et al., 2002)

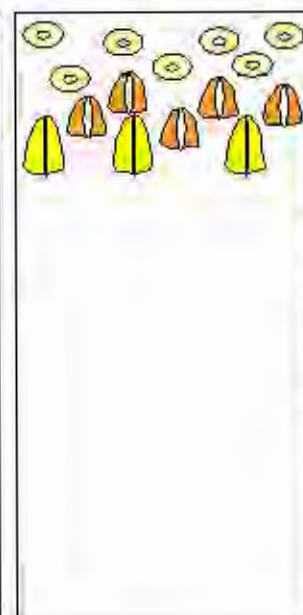
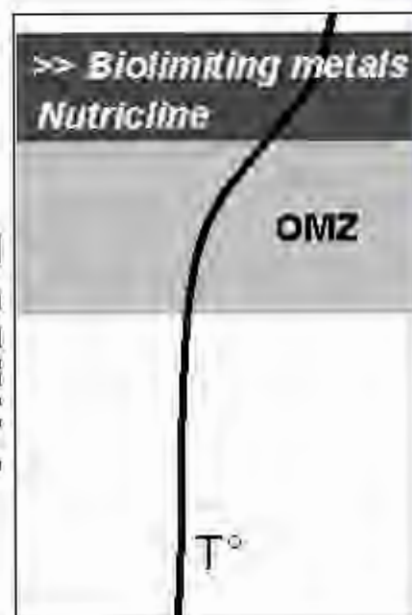


Phase 3



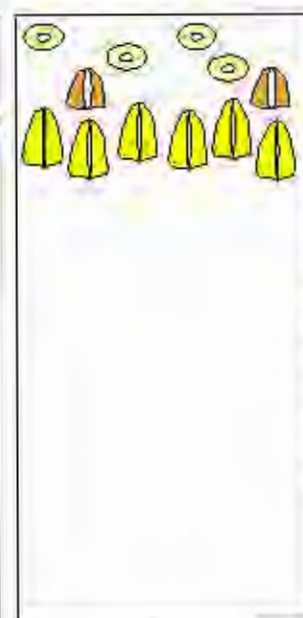
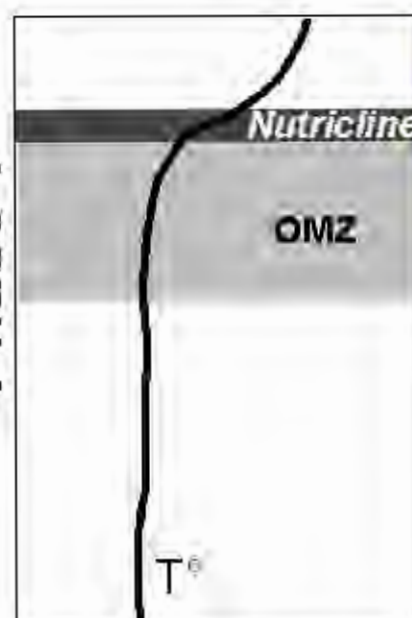
**121 Ma
Onset of OAE1a**

Phase 2








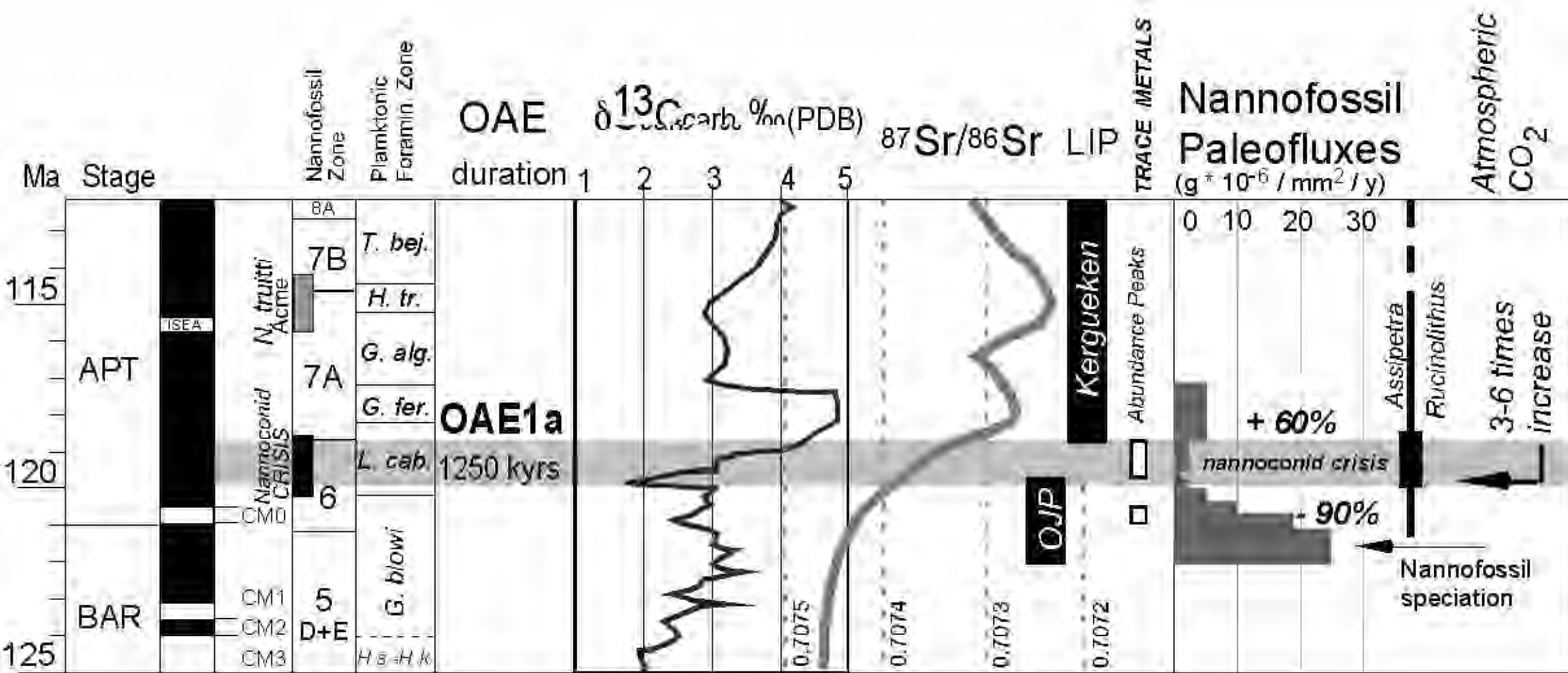
**121 - 120.5 Ma
CM0**

Phase 1



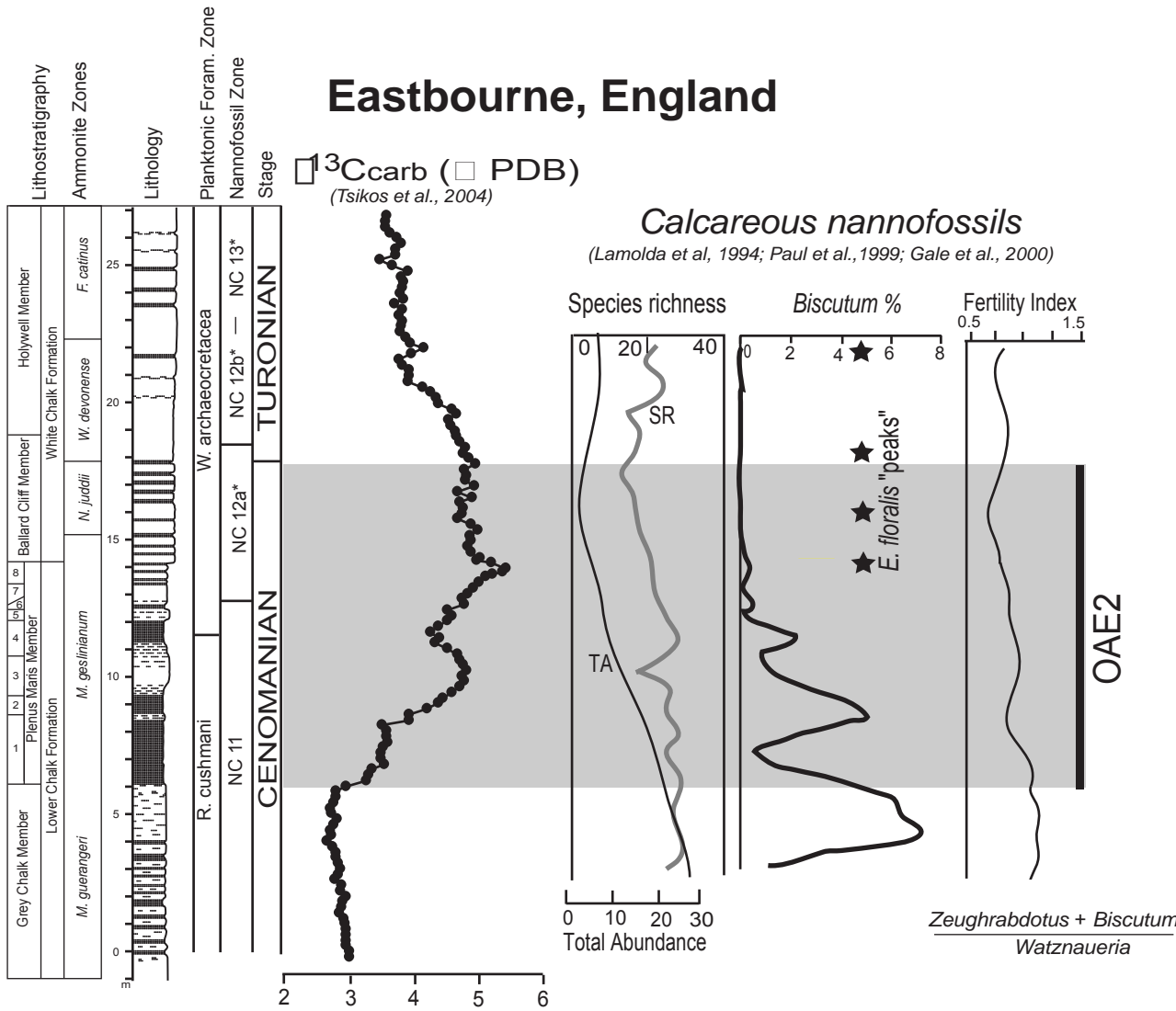
**124 - 121.5 Ma
Late Barremian**

-  narrow-canals nannoconids
-  wide-canals nannoconids
-  coccoliths
-  dinoflagellates
-  cyanobacteria
- OMZ = oxygen minimum zone

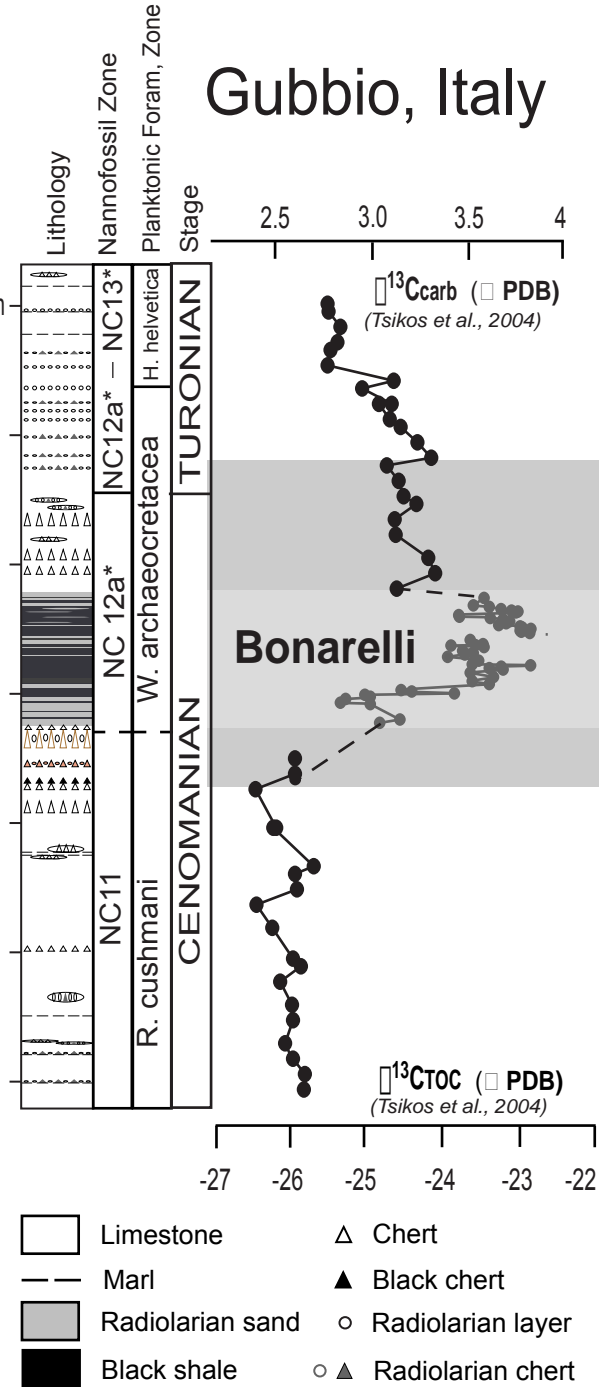


Erba - Figure 4

Eastbourne, England

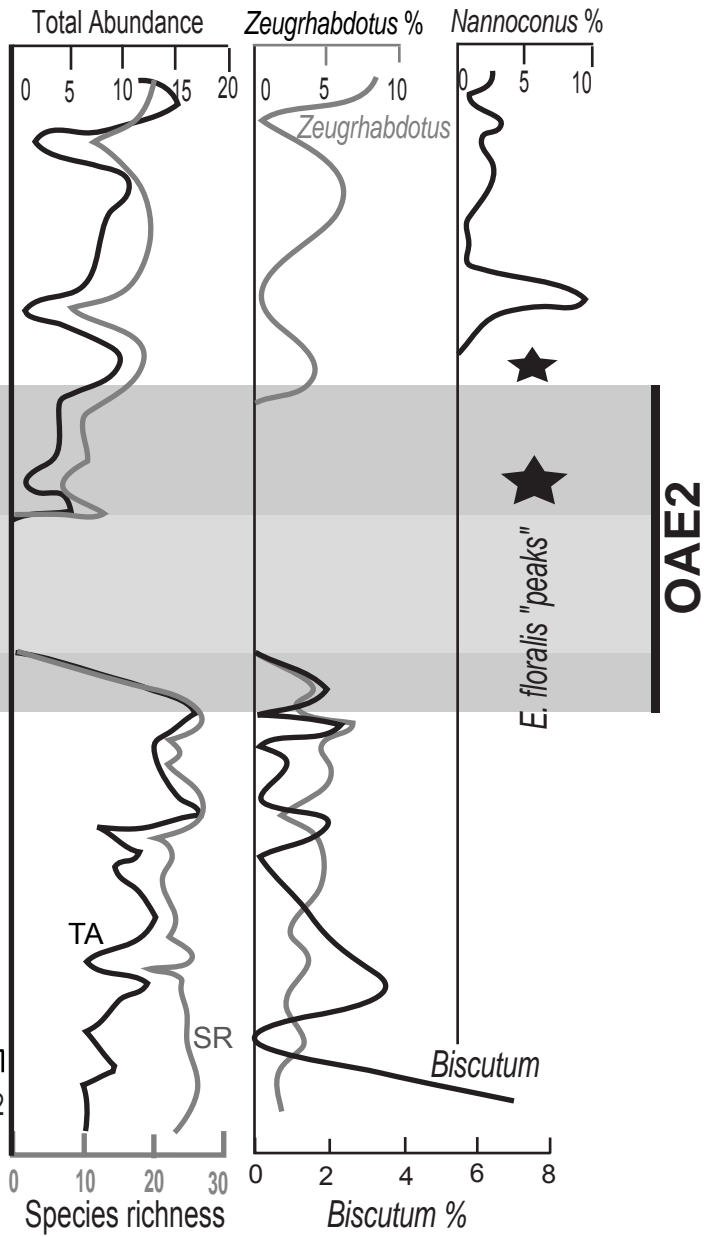


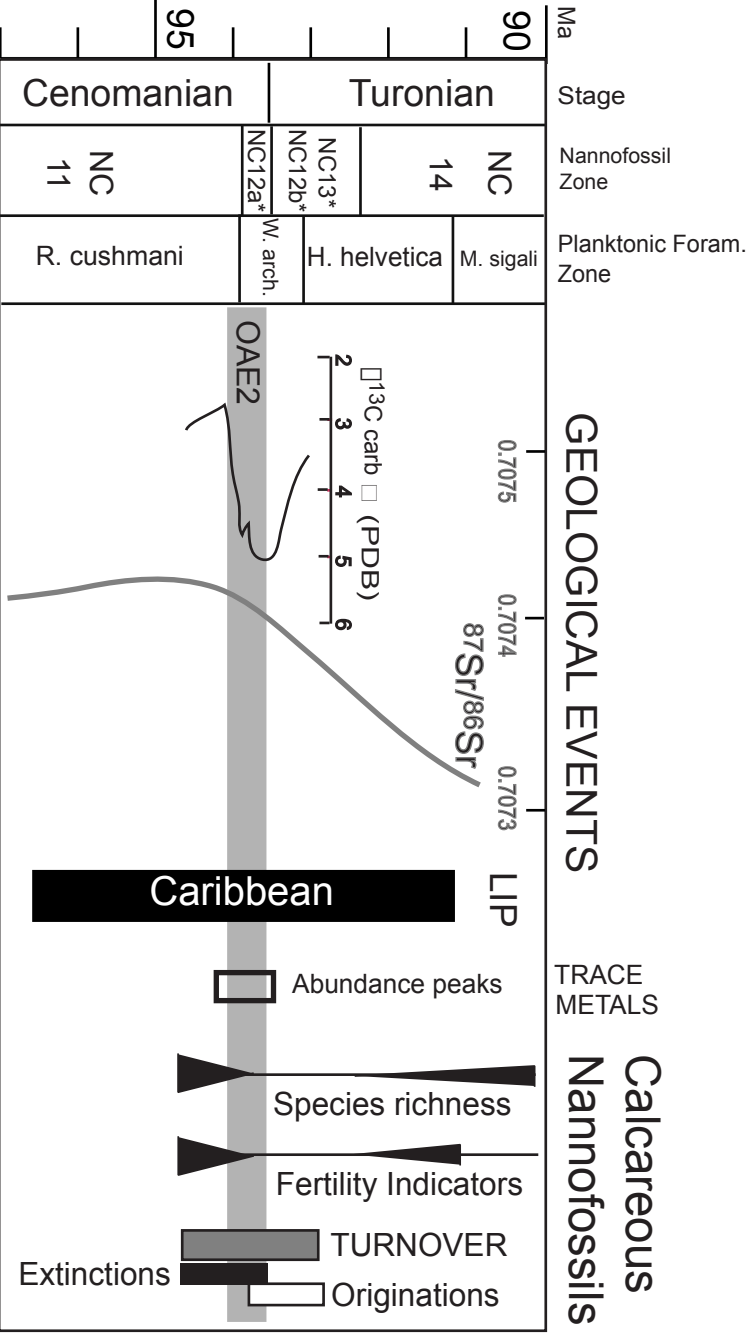
Gubbio, Italy



Calcareous nannofossils

(Erba, this paper)

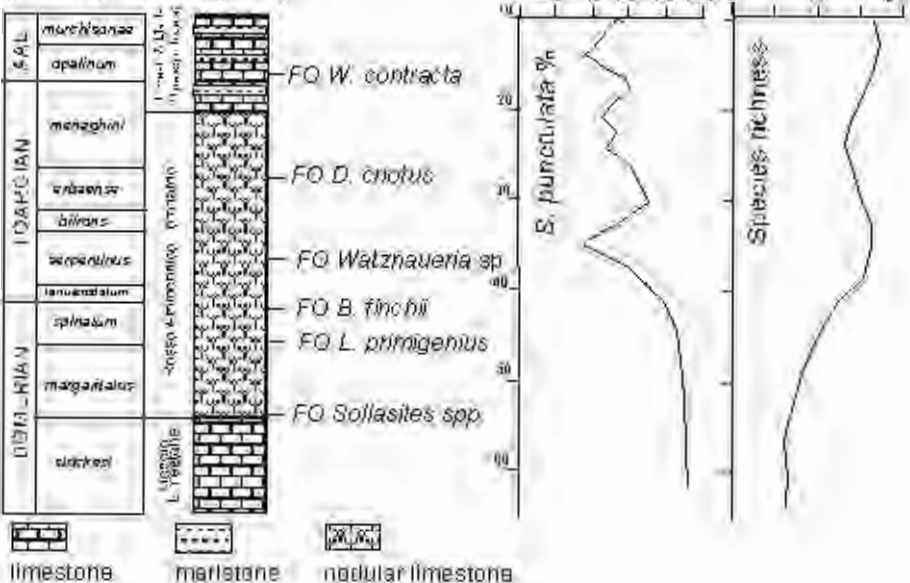




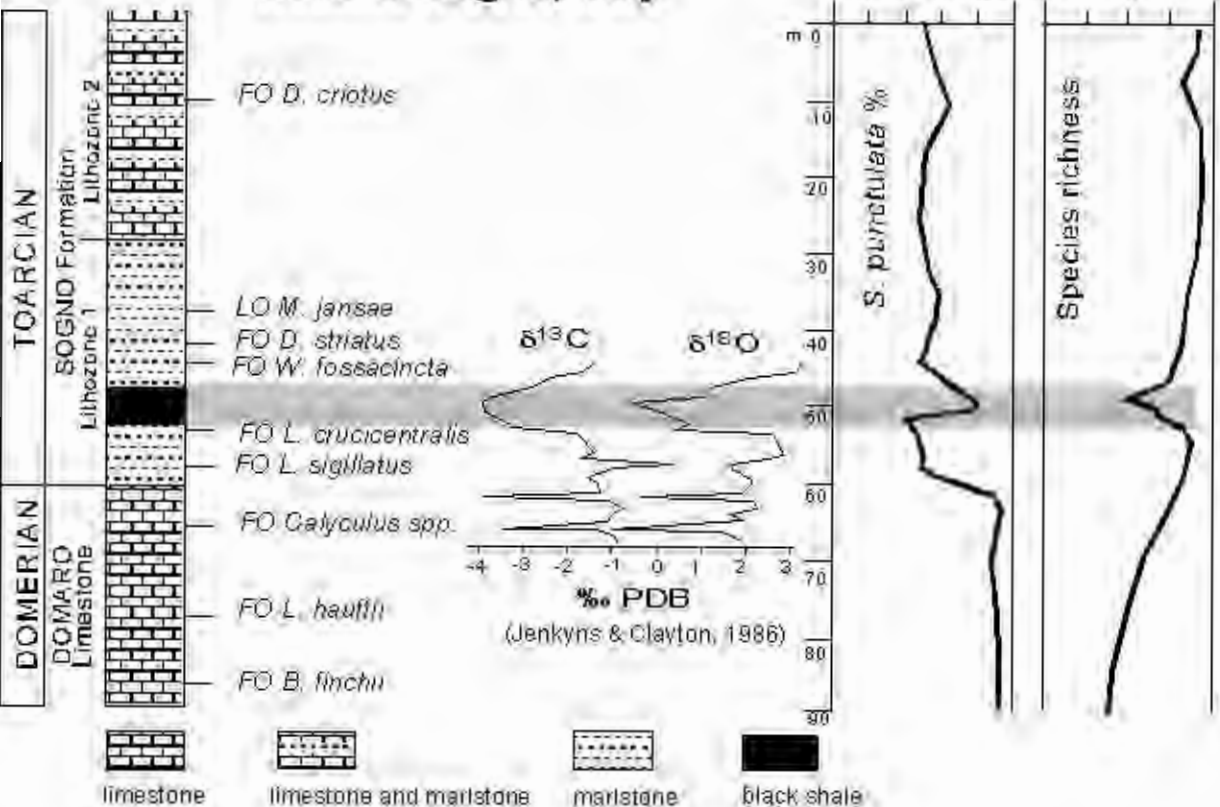
Erba - FIGURE 7

Breggia, Switzerland

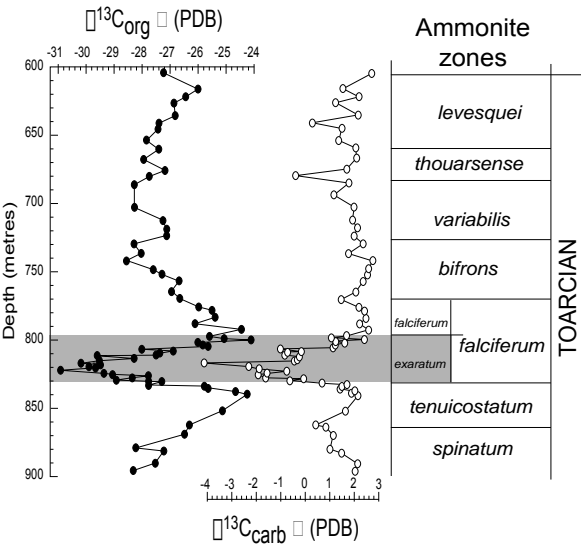
(Picotti & Cobianchi, 1996)



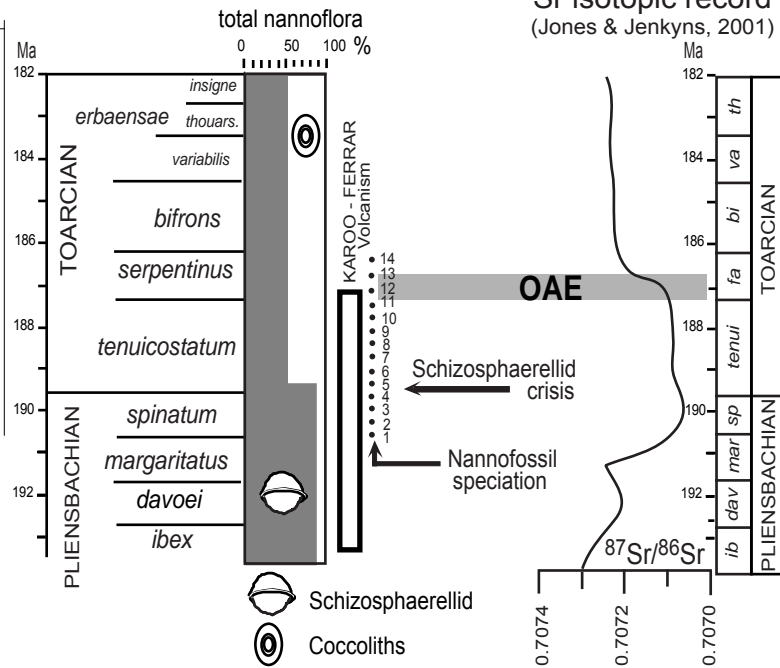
Colle di Sogno, Italy



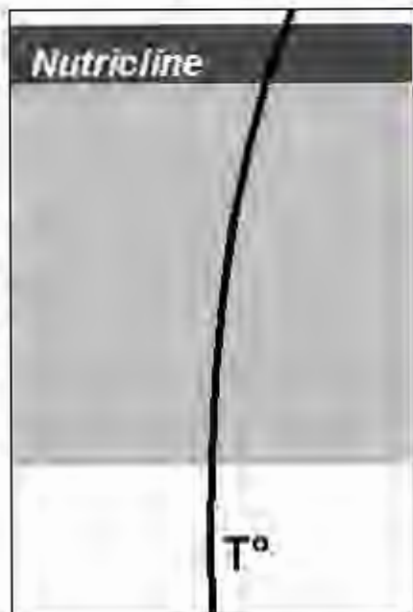
Mochras Farm borehole, Wales
(Jenkyns et al., 2002)



Southern Alps, N Italy

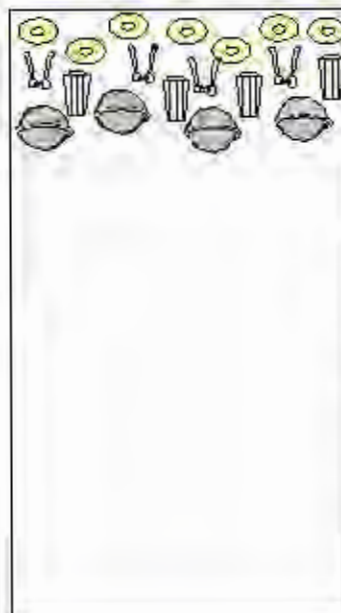
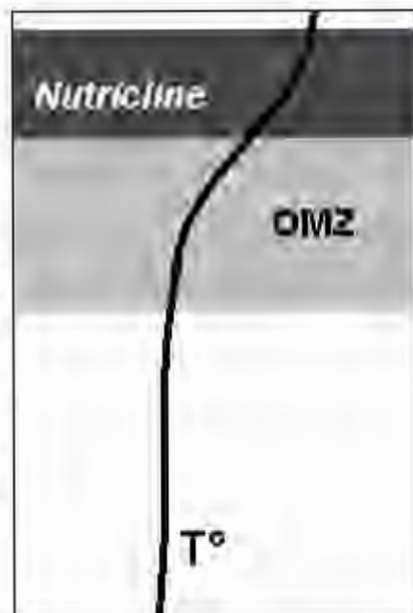


Phase 3



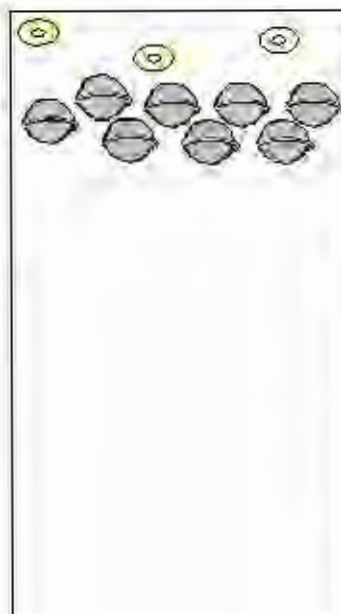
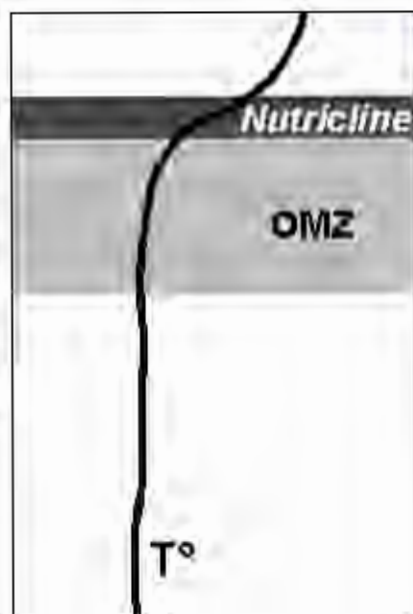
OAE *falciferum* Zone

Phase 2



tenuicostatum Zone

Phase 1



spinatum Zone

- coccoliths
- Mitrolithus*
- Calyculus*
- schizosphaerellids
- Tasmanites*
- cyanobacteria

OMZ = oxygen minimum zone

